TÉCNICO LISBOA

Ball Handling Mechanisms for Mobile Robots

Miguel Santos Serafim

Thesis to obtain the Master of Science Degree in

Electrical and Computer Engineering

Examination Committee

Chairperson: Prof. João Manuel Torres Caldinhas Simões Vaz

Supervisor: Prof. Pedro Manuel Urbano Almeida Lima

Members of the Committee: Prof. Maria Beatriz Mendes Batalha Vieira Vieira Borges

October 2013

Acknowledgments

First, I would like to thank Professor Pedro Lima, my supervisor, for the guidance and opportunity of working in the SocRob team under such an interesting and fun subject. It was very rewarding to work as part as a team, for the experience received and good working environment.

Secondly I would like to thank all the SocRob team members for the help and welcoming environment. With especial thanks to João Sousa who was responsible for bringing me to the team and was always available to discuss ideas. And to João Reis, João Messias and Pedro Santos who helped me integrate my work in the SocRob robots.

I would also like to express my deepest gratitude to Professor Maria Beatriz Borges for being my teacher during my academic journey and for the help during the development of this thesis.

I am also thankful to all my friends who made this academic years much easier and helped me get this far. Their constant presence helped me relax with countless great moments.

Finally and most important of all, a big thanks to my parents for all the support, motivation and patience through the years. Without them none of this would have been possible.

Abstract

This thesis addresses the use of ball handling mechanisms by soccer robots. In order to provide a quality match similar to a real soccer game, these mechanisms are essential for the robot to be able to control the ball, turning cooperation between robots and goal scoring possible.

Two different systems were developed, one to kick the ball and another to help the robot move through the field without losing the ball.

The kicker system consists of an electromagnetic actuator, comprising a power converter (current-mode boost converter), and a solenoid which converts the electrical energy stored in $100V$ capacitors into the movement of a plunger (kinetic energy). The studied system plans to reach up to $9m/s$ shots.

The dribbling system is achieved by installing a motor and a wheel that acts on the ball keeping it always in the possession of the robot.

The systems are developed from theory to practice, and the SocRob platform is used to test the results using both systems.

Results show that the systems were able to perform their duties, the kicker prototype shot the ball with the expected velocity ($5.5m/s$), indicating that the studied simulations are representative and the new model will be able to achieve the simulated results ($9m/s$). The dribbler has greatly improved the robot performance with the ball when compared to its previous state, giving the ability to move forward and stop without losing the ball, dribble backwards and perform turns and rotations with higher success rates.

Keywords: Robot soccer, electromagnetic actuator, boost converter, ball handling, ball dribbler, ball kicker.

Resumo

Esta dissertação estuda o uso de mecanismos para o controlo de bola por parte de robôs próprios para jogar futebol. A fim de proporcionar uma qualidade de jogo semelhante á realidade, este tipo de mecanismos é essencial para que os robôs consigam controlar a bola, e para que a cooperação entre robôs e a marcação de golos seja possível.

Dois sistemas distintos foram desenvolvidos, um com o intuito de chutar a bola e outro com o objetivo de controlar a bola durante a movimentação do robô.

O sistema de remate consiste num atuador eletromagnético, constituído por um conversor de potência (conversor elevador controlado em corrente), e um solenoide que converterá a energia elétrica armazenada em condensadores de 100V, no movimento de um êmbolo (energia cinética). O sistema de remate estudado visa conseguir remates até 9m/s.

O sistema de drible é conseguido através da instalação de um motor e roda que atuam sobre a bola mantendo-a sempre na posse do robô.

Os sistemas são desenvolvidos desde a teoria até aos protótipos e a plataforma de robôs de futebol (SocRob) é utilizada para testar os resultados com os sistemas em uso.

Os resultados mostram que os sistemas desenvolvidos foram capazes de desempenhar as suas funções, o protótipo do sistema de remate conseguiu chutar a bola perto da velocidade estimada (5.5 m/s), indicando que os melhoramentos simulados são representativos e o novo modelo será capaz de atingir as velocidades simuladas (9 m/s). O mecanismo de drible melhorou bastante o desempenho do robô com a bola comparativamente ao funcionamento sem sistema de drible, dando a possibilidade de driblar para a frente e travar sem perder a bola, driblar para trás e executar curvas e rotações com uma maior taxa de sucesso.

Palavras-chave: Futebol robótico, atuador eletromagnético, conversor elevador, controlo de bola, sistema de drible, sistema de remate.

Table of Contents

Index of Figures

Index of Tables

List of Symbols

V	Voltage [V]
L	Inductance [H]
i	Current [A]
D	Duty cycle
T_s	Period [s]
R	Resistance [Ω]
λ	Flux Linkage [Wb]
N	Number of turns
I	Current [A]
l	Coil length [m]
μ	Magnetic permeability [H/m]
A	Section of the coil [m^2]
H	Magnetic Field [A/m]
B	Magnetic flux density [T]
Φ	Magnetic flux [Wb]
$\Re$	Magnetic Reluctance[H^{-1}]
x	Distance [m]
a	Acceleration [m/s^2]
t	Time [s]
v	Velocity [m/s]
W	Work [J]
C	Capacitance [F]
m	Mass [kg]
τ	Torque [$N.m$]

I	Moment of inertia [$kg.m^2$]
α	Angular acceleration [rad/s^2]
r	Radius [m]
RPM	Revolutions per minute

Chapter 1

Introduction

The main goal of this chapter is to provide the context of this thesis, explain the motivation and problems behind this research work and, finally, state the thesis objectives. Additionally, the organization of the thesis is also reported.

1.1 Context and Motivation

As the interaction between mobile robots and the real world is becoming more and more important, being capable of handling objects as a human would do is a required feature of such robots.

In RoboCup [1], there are many challenges fostering robotics and AI research. One such challenge is RoboCup Soccer which is seen worldwide as a benchmark in robotics and has seen many important improvements in recent years. RoboCup proposed a future goal to be shared by all roboticists so they can all evolve and guide themselves towards a common objective, that is, “By mid-21st century, a team of fully autonomous humanoid robot soccer players shall win the soccer game, comply with the official rule of the FIFA, against the winner of the most recent World Cup.” [2], therefore, this league can be compared with a former goal that also took 50 years and was achieved by the supercomputer “Deep Blue” winning a game of chess against the world champion at that time, Garry Kasparov.

RoboCup Soccer has multiple leagues, as the Small Size League that features small wheeled robots controlled through computers and cameras on the field. The Middle Size League (MSL) where every robot is a complete player with vision and processing power. And there are the new humanoid leagues where the humanoid motion problems are being solved. All of these leagues have the purpose of sharing knowledge and in the future merge themselves to achieve their final common goal.

The MSL is the main event of RoboCup because it is where the robots have full onboard autonomy, every robot is an agent that has its own knowledge collected by the sensors equipped within the robot (e.g. omnidirectional cameras, compass, and accelerometers). Each robot has to self-localize on the field, localize the ball, and share its knowledge that may or may not be correct. This decentralized control makes this league the closest to a real game of football where every player plays according to its perception of the world and built-in plan.

In recent competitions the robots had a significant improvement in the way they interact with the ball. New systems provided the ability to kick and the ability to dribble much more efficiently. This improvement turned the game much closer to our idea of football, and spectators can clearly see in the game and by the final score, the difference in performance of a team with this kind of systems. Every year the rules of the league change in order to force the teams to be closer to the final objective, and since 2012, the rules changed so that players had to make much more use of passes between players by inserting a rule that prohibits a player from crossing the midfield line with the ball. Robots must now pass to a player in the opponent side of the field. This way, without a proper kicking device, it is very difficult to score or complete the passes that are required to comply with the rules.

These particular systems were missing in our robots and thus our team (SocRob) was unable to show good competition results and compete with high tier teams that possess this ability. As a requirement to continue with our team in competitions, it was necessary that such systems were developed and this thesis reports the work done in that direction.

1.2 Objectives

In the past, the SocRob team had systems to handle the ball, but they were never effective and seldom worked throughout the whole game. The objective of this thesis is to develop a fully functional kicker and dribbler system for the SocRob team. With this purpose in mind, the following tasks were defined.

1. **Analysis of other systems in RoboCup –** Initially, the previous systems of the team are analyzed as well as systems from other teams, so that the system that best served the objective and at the same time recycled components from our previous systems could be chosen.
2. **Development of the kicker system –** An electromagnetic kicker is developed with major improvements in the step up converter and electronics, and then tested and optimized. The developed kicker should be able to kick the ball with velocities close to $10 m/s$, as well as slower passes.
3. **Redesign of the dribbler system –** The dribbler system is redesigned to overcome the errors detected in the previous system. The dribbler system must be able to drive the ball and help the robot complete its tasks.
4. **Assembly of both systems in a SocRob robot –** Both systems are assembled in a SocRob robot and the performance is evaluated in full robot operation.

In summary, it is expected that the robot will be able to do repetitive kicks at the ball with different speeds and has a greater ability to drive the ball across the field.

1.3 Contributions

The work developed under this thesis, equipped the SocRob soccer robots with an electromagnetic linear actuator exploring a different approach regarding the power converter. A current-mode boost converter is implemented resulting in a fast and secure charging system.

Regarding the electromagnetic actuator an extensive magnetic analysis on how to optimize the solenoid is explained.

Additionally, a dribbler system is developed and tested to study the viability of using a low cost dribbler to help a soccer robot perform its main tasks.

Both systems were equipped on the SocRob robots which are now able of new cooperative behaviors, opening new opportunities in research.

1.4 Thesis Structure

This thesis is organized in six chapters, including this first chapter that features an introduction and context of this thesis.

Chapter 2 presents the restrictions faced due to Robocup MSL rules, the robot platform on which this work will be implemented, the former actuators used to handle the ball, and a review of the state of the art in this kind of actuators.

In Chapters 3 and 4, a kicker system and a dribbler system are presented respectively. Both chapters begin with a theoretical introduction and basic principles of the systems, then all the development process, including sketches and simulations, and finally the results of the tests will be presented.

Next, Chapter 5 reports the work done integrating the systems with the SocRob robots, and shows the final results.

Finally, in Chapter 6, the conclusions, achievements and possible future improvements are presented.

Chapter 2

Background

The main objective of this chapter is to review the conditions imposed by the RoboCup MSL rules [3], introduce the SocRob robot platform, and analyze the former handling mechanisms and the state of the art systems, guiding the development of the new devices.

RoboCup MSL is a league for soccer robots playing with a FIFA standard size 5 football that has more or less 22cm of diameter, and this year it is dimensioned for 5vs5 players in a field of 18mx12 m, these dimensions are enough so that players can take advantage of long passes throughout the field, and for that, the kicker system has to be able of relatively powerful shots as well as measured and precise passes (whose strength may depend on sensed information, such as the distance to the receiving robot).

There are a set of rules related to the robot geometry and ball manipulation from which the ones relevant in the scope of this thesis are:

RC-4.2.0: Robot Size

- "The maximum weight of a robot is 40kg."
- "Each robot must possess a configuration of itself and its actuators, where the projection of the robot's shape onto the floor fits into a square of size at least 30cm × 30cm and at most 52cm × 52cm."

RC-12.0.1: Ball Manipulation

- "During a game the ball must not enter the convex hull of a robot by more than a third of its diameter except when the robot is stopping the ball. The ball must not enter the convex hull of a robot by more than half of its diameter if the robot is stopping the ball. This case only applies to instantaneous contact between robot and ball lasting no longer than one second. In any case it must be possible for another robot to take possession of the ball."

- “The robot may exert a force onto the ball only by direct physical contact between robot and ball. Forces exerted onto the ball that hinder the ball from rotating in its natural direction of rotation are allowed for no more than one second and a maximum distance of movement of one meter. Exerting this kind of forces repeatedly is allowed only after a waiting time of at least four seconds. Natural direction of rotation means that the ball is rotating in the direction of its movement.”
- “Ball rotation also implies that the ball is rotating continuously, even if slightly slower than its natural rotation speed. Movements of the ball such as “roll-stop-roll-stop” are not considered a valid ball rotation and will be considered ball holding.”
- “Dribbling the ball backwards, that is, dribbling while the robot is moving towards the opposite direction of its relative position to the ball is allowed for a maximum distance of 2 meters. During the backward dribble the ball must also be rolling in its natural direction. Once any particular robot has dribbled the ball backwards for more than 1 meter, it cannot repeat the same backward dribbling again before the ball has been completely released by that robot or until the robot has engaged a new ball struggle against an opponent robot (i.e. the ball is actively disputed between the two opponent robots for more than 2 seconds).”

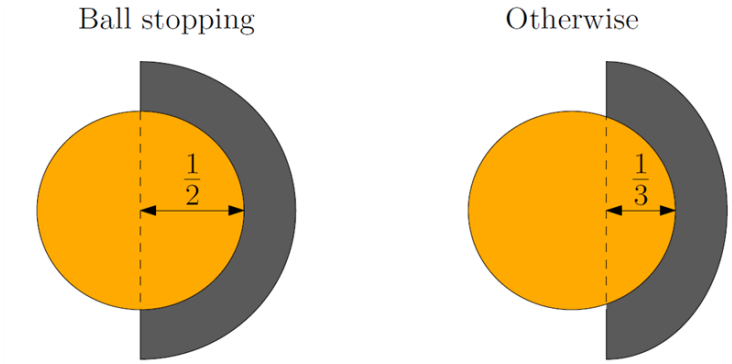

Figure 2.1 - Ball/Robot restrictions [3]

These are the rules for this year official competition and development should have in consideration that future competitions will evolve for bigger fields and situations closer to actual 11vs11 football games.

2.1 State of the Art

There are several kicker and dribbler systems already in use by other teams in RoboCup, a survey is available in other studies [4]. Here, the main types of kickers and dribblers will be presented, followed by a comparison and a deeper presentation of the most remarkable systems.

Kicker Systems

The Kicker systems developed by RoboCup MSL teams can be classified as:

- **Spring based:** this system can use a motor or any other device to generate a mechanical force to compress a spring and store that energy by locking the system in a high energy state. When it is desired to kick the ball, the spring is unlocked, releasing its energy. This

system usually takes a lot of space inside the robot, and it is difficult to shoot with different speeds, so this system was dropped by most of the teams because of the changes in the rules that required passes between team members. Teams who used this system were SocRob (Figure 2.2) and Hibikino-Musashi [5] from Japan.

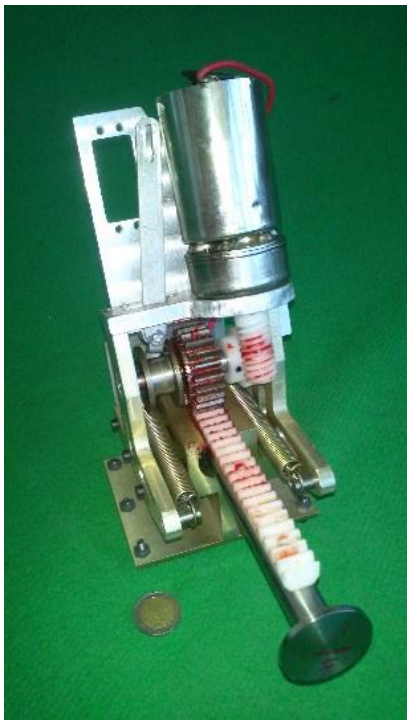

Figure 2.2 - Spring based kicker system from SocRob, IST

- **Pneumatic:** this one uses a compressed air tank as a power source to produce the kick. It is the simplest of the three systems, as it simply has pneumatic valves connected to the tank, and by controlling the valves one chooses when to shoot. The disadvantages are that the number of shots one can do are very limited by the size of the air tank, and the speed of the kicks cannot be controlled. SocRob had a system like this in 2002-4. An example of a pneumatic system can be seen in Figure 2.3.

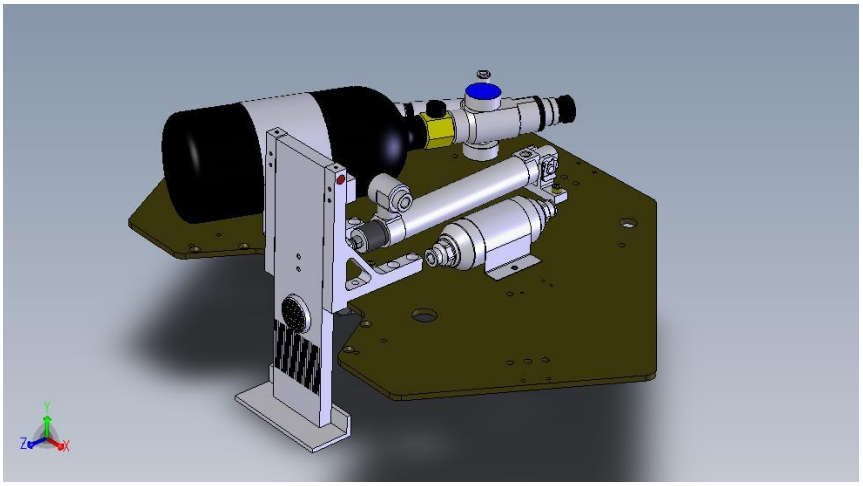

Figure 2.3 - Pneumatic kicker system from "OpenTribots" [6], Freiburg University.

- **Electromagnetic:** which uses a coil with a magnetic plunger inside. When a current is applied to the coil, the plunger accelerates towards the ball. This type of system is referenced as being the best for the application considered here and is being adopted by most of the teams, including the top tier. Usually energy is stored in capacitors at a higher voltage, because the voltage from the batteries cannot produce a proper kick. The discharge time can be controlled to produce kicks with different speeds, and the time required between two kicks is relatively short taking into account the application. The disadvantage of this method is that using high voltages is dangerous, but this can be solved by having everything well packed.

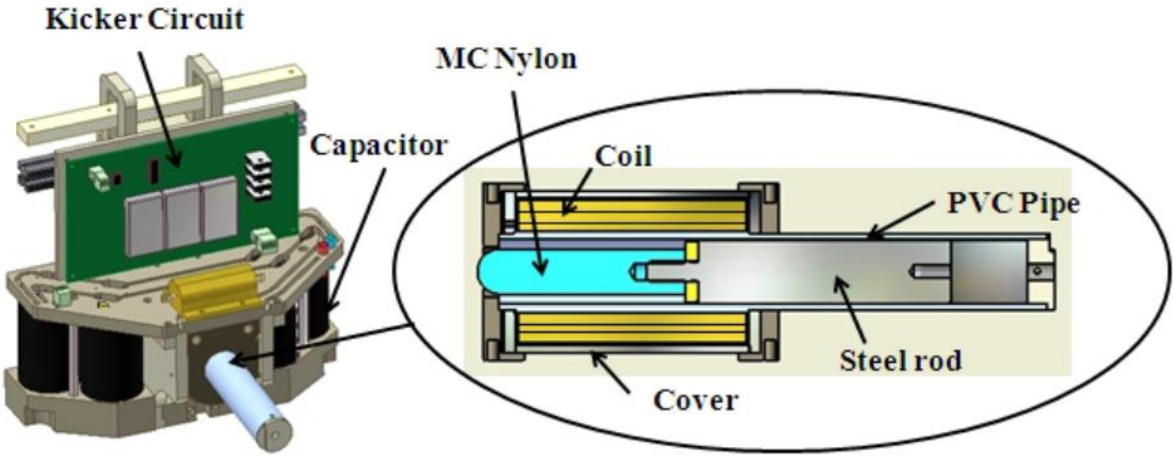

Figure 2.4 - Electromagnetic Kicker System from Hibikino-Musashi [7], Japan

After listing the different solutions, a comparison of each of their properties highlights the pros and cons of each mechanism.

The properties of interest are, in order of importance:

- Shooting power – The kicker has to, at least, be able to produce long shots.
- Cost – The price range must be reasonable in the scope of the project.
- Simplicity – The system should be mechanically simple reducing the need of repairs and maintenance.
- Power modulation – Shots and passes with several strengths must be possible.
- Weight and size – The robot has limitations in size and weight that must be respected.
- Time between shots – Fast recharge times are needed so the robot may repeat a kick faster.
- Number of shots – Ability to kick the ball during the whole game should be met.
- Safety – The robot must be safe for team members, RoboCup staff and supporters.

As seen in Table 2.1, the solenoid approach is the best option and only loses to other solutions in the safety category because of the use of high voltages.

Table 2.1 - Comparison of kicker mechanisms [4]

Properties	Spring	Pneumatic	Solenoid
Shooting power	+	-	+
Costs	+	+	+
Simplicity	-	+	+
Power Modulation	-	0	+
Weight	-	+	+
Space Required	-	-	+
Time between shots	-	+	+
Number of shots	+	-	+
Safety	+	+	-

A good example of kicker system is the one used by “Tech United” [8], they currently use an electromagnetic kicker capable of shots as fast as 11.2m/s using the energy stored in a 4.7mF 450V capacitor. Their time for a complete charge is about 15 seconds. And they can not only do lob shots, but also choose the angle at which the ball is fired, having their solenoid coupled to a movable leg. Both adjust to hit the ball in the desired place. Figure 2.5 illustrates their system.

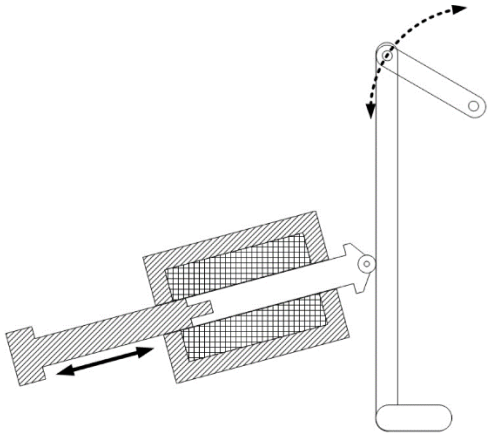

Figure 2.5 - "Tech United" lob shot system [8]

Dribbler Systems

Regarding dribbling systems, two categories can be found:

- **Passive Systems:** which act as guides so the ball won't drift away during dribble maneuvers, in this kind of system the ball rotates freely in front of the robot. The flaw of these systems is the impossibility of dribbling backwards or to perform more aggressive movements. The robots must rely on path planning strategies to control the ball and this reduces a lot the results during the competitions. Examples of this approach are the "OpenTribots" [6] that use folded rubber supports and the "Hibikino-Musashi" [7] team that uses rubberized arms controlled by a motor. Both systems can be seen in Figure 2.6.

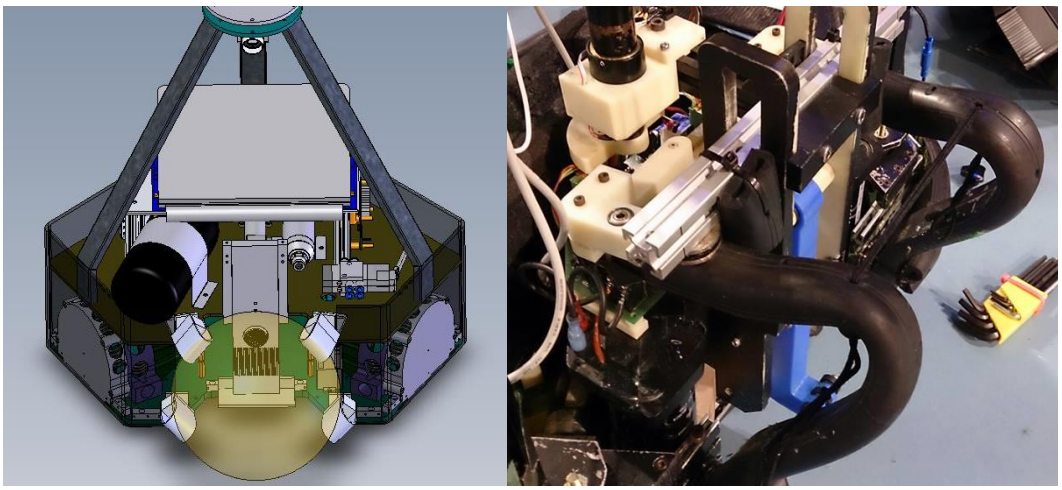

Figure 2.6 - Passive Dribbler Systems, (Left)"OpenTribots" [6], (Right) "Hibikino-Musashi"

- **Active Systems:** use motors coupled to wheels with an adherent surface, in the front of the robot. This wheel is used to force the ball into rotating in the desired direction. This way the ball moves according to the rules and the robot is able to pull the ball to move backwards or can momentarily hold the ball in difficult situations like fast change of directions or a scrum between robots. With this kind of systems, some teams can have a tighter control than others, inducing the ball to rotate substantially slower than the expected and this can give an unfair advantage against better systems closer in spirit to the rules. Most teams use active systems due to the higher performance achieved, adding different mechanical approaches and sensors to help track the ball. Differences range from simple and efficient one-wheel solutions as the one "CAMBADA" [9], from University of Aveiro, used last year, to the more advanced two tilted wheels used by "Tech United" [10] from Eindhoven University of Technology. "CAMBADA" recently changed to a system like this. Both systems can be seen in Figure 2.7 and Figure 2.8.

Figure 2.7 - "CAMBADA" dribbler system from 2012 [9]

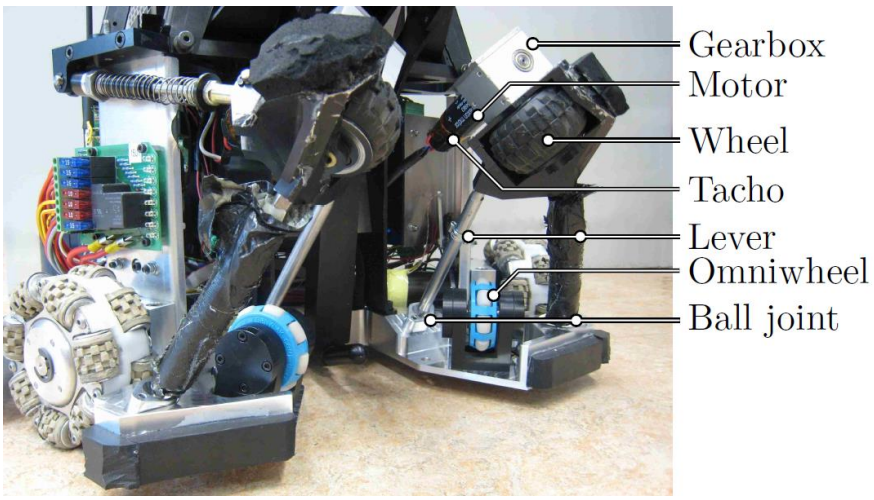

Figure 2.8 - "Tech United" dribbler system [11]

Amongst the most advanced dribbler systems, we should point out the "Tech United" dribbler system [11] which uses two top wheels doing the main work that is push or pull the ball and can also force the ball rotate left or right. The wheels are driven by Maxon RE25 20W DC motors and located at the end of levers that move back and forth to adjust to the ball and attenuate frontal impacts. Also, these levers have a potentiometer attached through a wire, providing feedback of the angle of the levers which can give an accurate knowledge of the ball position. Adding to this, the robot also has another pair of omniwheels on the bottom, which purpose is to maintain a fixed minimum distance between the robot and the ball and avoid climbing over the ball when it gets stuck and the top motors continue pulling. This system with which they won the 2012 world championship was recently improved. The team modified the position of the wheels and levers putting them further apart and higher, and according to their results the robot was able to catch incoming balls with a misaligned angle of almost 30º degrees or 15cm of translational offset [12].

2.2 SocRob Omni

In 2006, the Institute for Systems and Robotics - Lisbon (ISR-Lisbon) acquired five robots [13] with the intention to participate in the RoboCup MSL league and for general robotics research. Nowadays, the robots are slightly different from the original ones. Some of the initial components were upgraded. At the time the robots consist of:

- A hollow aluminum chassis, with the complete robot projection on the floor fitting a $48cm \times 48cm$ square.
- Two $12V$ NiMH $10Ah$ batteries to power the robot.
- 3 Omnidirectional wheels powered by MAXON DC motors (RE35/118776), with a gear ration of 91:6 (MAXON 203116).
- A network camera with fisheye lens, that is located in the top of the robot, facing down, enabling a 360º surround view. The camera is used for the robot ball detection and self-localization algorithms.
- A compass (HMC6352), to help with localization.
- A microcontroller (Arduino Duemilanove [14]), to control the electronic sensors and actuators at a low level stage.
- A Laptop, for high level tasks, image processing and wireless communications.

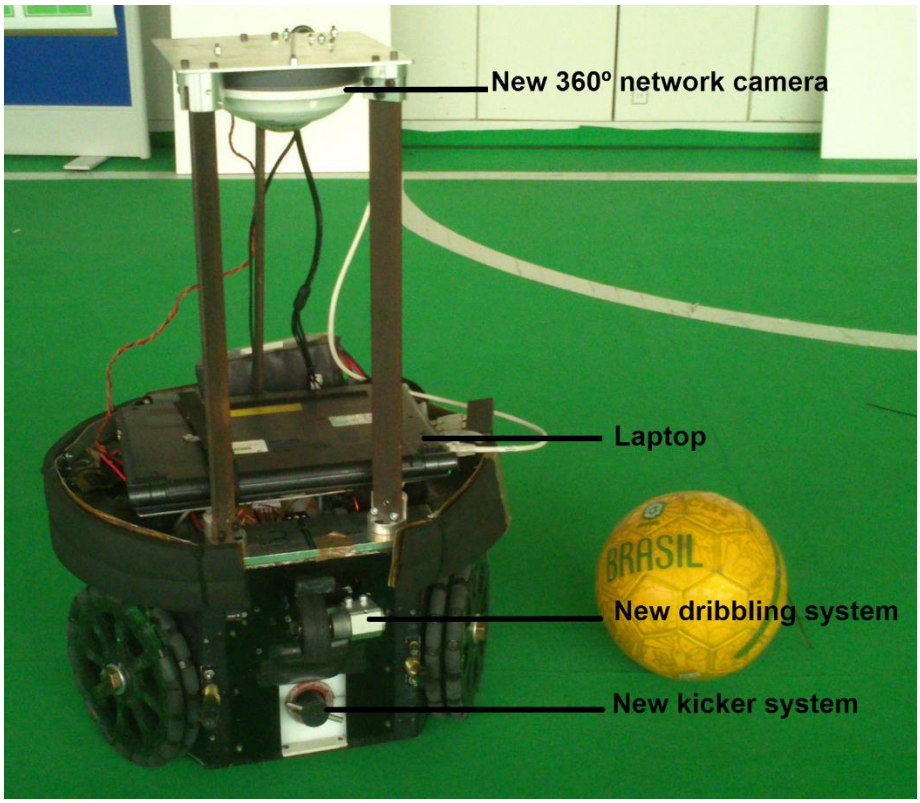

Figure 2.9 - Current SocRob robot

The original robot was equipped with both a kicker and a dribbler system,

- The original kicker system used the spring approach and was dropped by the team. Later the team started the development of an electromagnetic kicker that had been installed

in the robot but never worked properly, the system lacked the ability to reach the right voltage on the capacitors and had problems regarding the discharge during the kick. Therefore being the electromagnetic kicker the system we intended to pursue, it was decided to continue the work in this system in order to use the same components, reducing costs. Though a deep analysis is needed to find the problems, so a new one could be designed without getting into the same mistakes.

- The original dribbler system consisted of a rolling drum in front of the robot that was driven by a motor inside the robot, thus the transmission of power was done through a belt. The mechanism also had a servo motor to change the height of the drum. At the time of this thesis all of these systems were severely damaged, and were not functioning, nonetheless one of them was repaired and tested to infer its performance. Several problems were encountered with the mechanism:
    - The system did not have proper protection or structural resistance for its use.
    - The belt in such extreme conditions frequently became loose.
    - The cylinder shape of the drum is a good choice, but the drum used did not have enough adherence to seize the ball.
    - The servo motor used to change the height of the cylinder, was not useful as the robot did not have time to react.
    - The system was only able to pull the ball, and the ball gets stuck when moving forward.

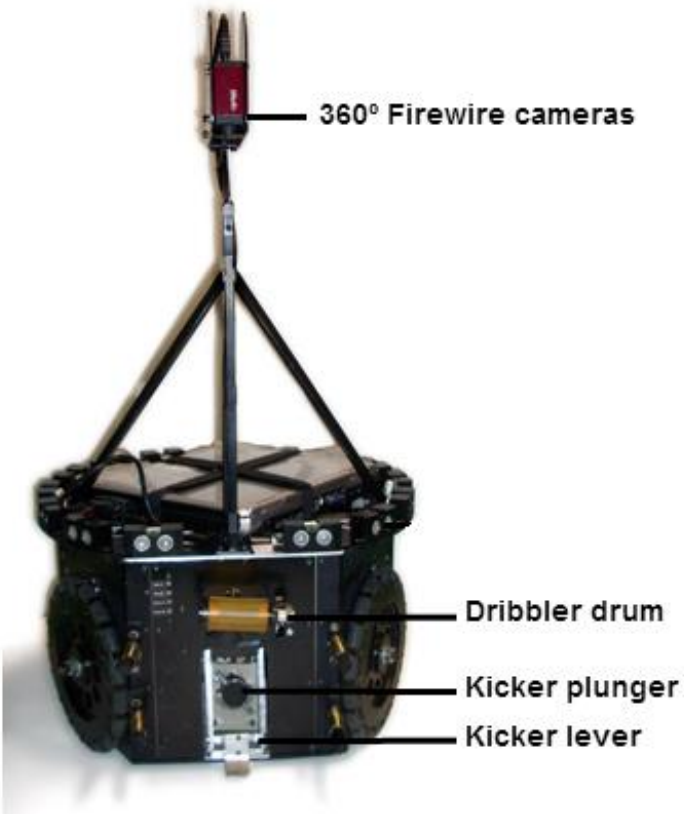

Figure 2.10 - Original SocRob robot with the older handling systems

Chapter 3

Kicker System

The basic principle behind the electromagnetic actuator is self-inductance, by passing a current through a turn of wire, a magnetic field is formed. With magnetism, magnetic materials can be attracted or repulsed. This actuator is basically a tube of non-magnetic material with several turns of wire (solenoid) to produce a big magnetic field, creating enough force to move a ferromagnetic projectile that is loose at the end of the tube.

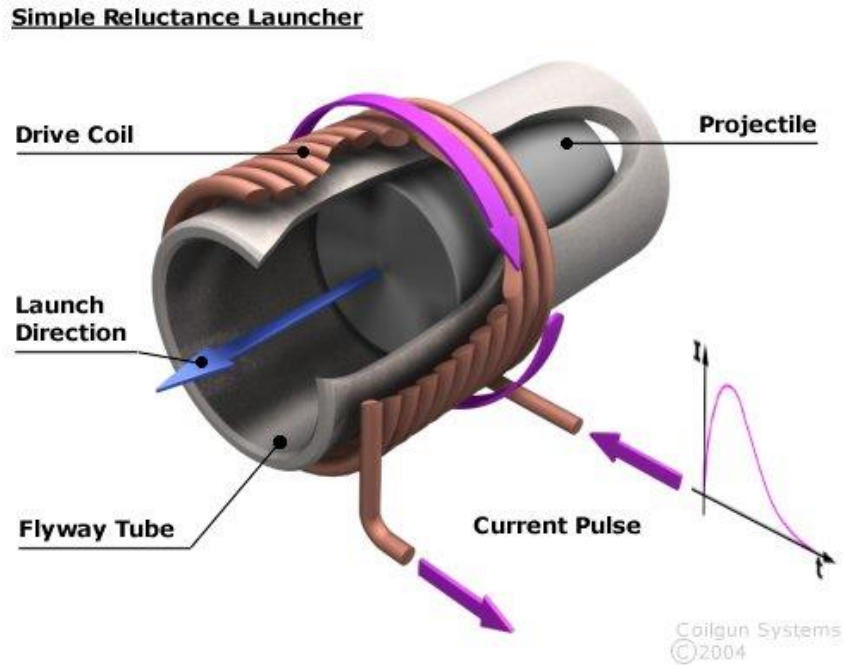

Figure 3.1 - Electromagnetic linear actuator [15]

The force exerted on the projectile (thrust rod), has to be strong enough to kick a ball, so, a high current is needed in the coil. For that the 12*V* available in the batteries are not enough and the batteries cannot draw the instantaneous current needed. This system has to be paired with a DC/DC power converter that will convert the voltage in the batteries to a higher voltage to be stored in capacitors. Then

the capacitors can be discharged through the coil, converting the electric energy stored in the capacitors into kinetic energy in the projectile.

The kicker development will be divided in two stages. The power converter will be presented in section 3.1. The developed power converter consists in a current-mode boost converter separated in two boards:

- The “ControlBoard” with the control electronics required for the current-mode operation.
- The “Boost PowerBoard” with the boost converter circuit that will be submitted to high currents.

The solenoid and the “Kickboard” that controls the discharge of the capacitors are explained in section 3.2.

The system has two levels of control, a high level running on the dedicated laptop of the robot, and a low level in a microcontroller that will interact with the electronic boards. A diagram explaining the architecture of the system is shown in Figure 3.2.

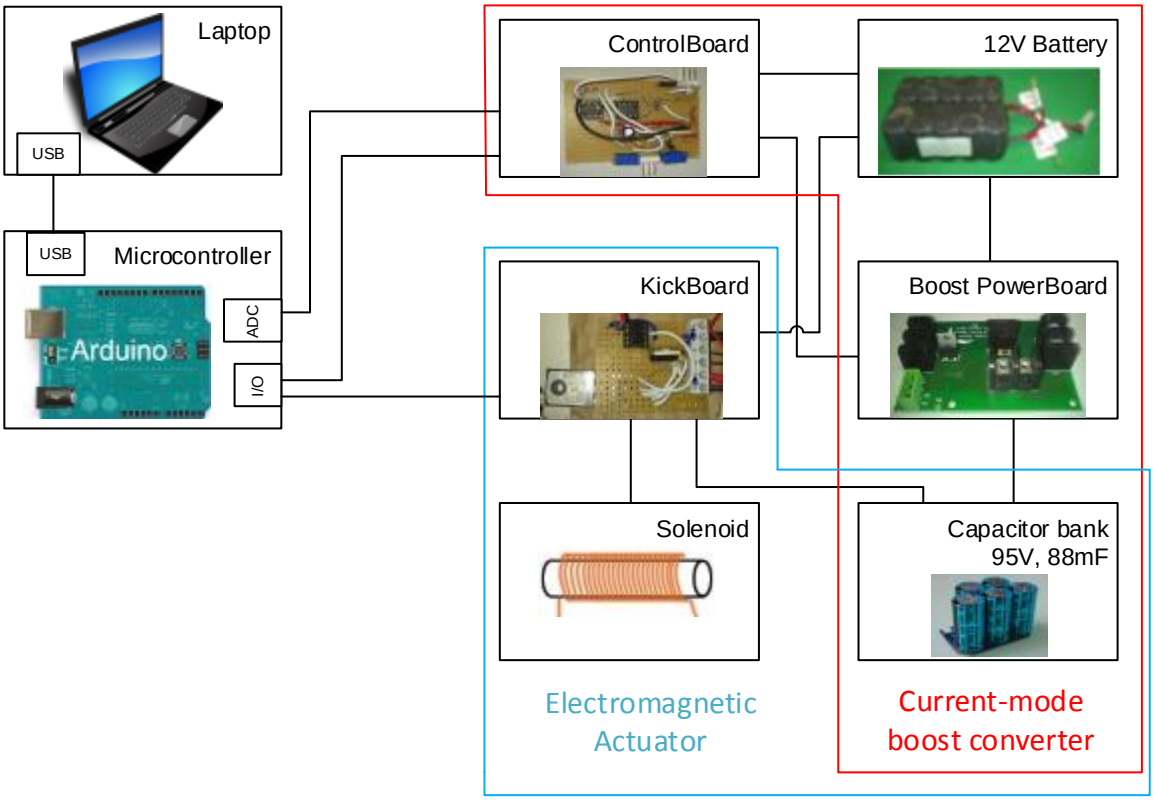

Figure 3.2 - Kicker system architecture diagram

3.1 Power Converter

There are several topologies for DC/DC power converters that can raise the voltage of the output. These are widely used to generate higher voltages with a drop in current because ideally the power drawn from the input must match the output, and so innumerous topologies are constantly developed, improving the efficiency.

In the scope of this project there is no need for power efficient topology, since the objective is to store energy in capacitors and there is no equilibrium in the output to be met. The output will be fully capacitive and won't consume energy when it's charging.

Many teams use a simple step-up converter (boost converter), and this topology is enough for the ratio of voltages intended (12V to 100V). The team already has 100V capacitors to use in the robots, and this is an expensive component, so, the capacitors will be used with a final voltage of 95V.

3.1.1 Theory

The boost converter [16] represented in Figure 3.3, is a switch mode DC/DC converter that works by switching between two states consistent with the transistor "on" and "off" state. While the transistor is "on", V_L is constant and i_L linearly ramps up, increasing the energy in the inductor.

$$V_L = L\frac{di_L}{dt} \tag{3.1}$$

Then by turning the transistor "off", the inductor will create a voltage V_L, to maintain the linearity of current, forcing the inductor current to flow through the diode, transferring some energy to the output.

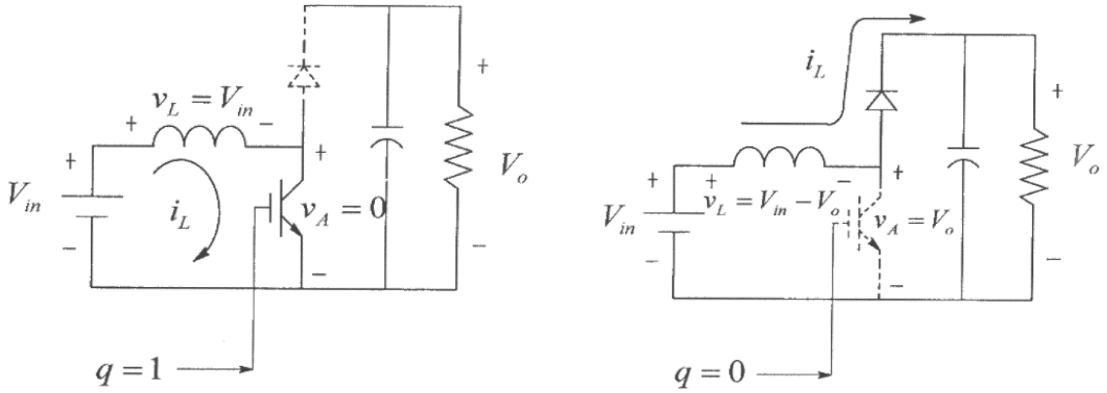

Figure 3.3 - (Left) Boost converter "on" state, (right) Boost converter "off" state [16]

To make it simpler to understand let's assume that the components are ideal and the converter is working in a steady state mode that is the continuous conduction mode (CCM). In this mode the converter operation is periodic, and there is always current in the inductor (i_L).

The converter waveforms are shown in Figure 3.4, where "D" represents the duty cycle at the gate of the power transistor, meaning that the transistor is "on" during "D" and "off" during "$(1 - D)$".

The inductor voltage (V_L) takes two values: V_{in} while it's "on". And $-(V_o - V_{in})$ while it's "off", this value is the sufficient so the diode becomes forward-biased.

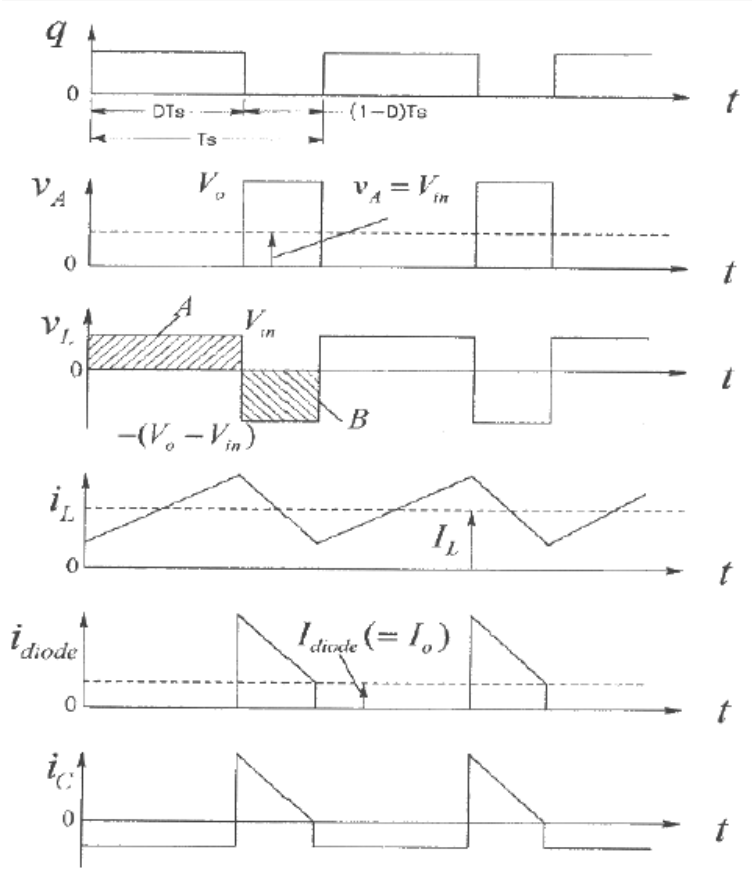

Figure 3.4 - Theoretical boost converter waveforms [16]

While in CCM, the area A and B from V_L are equal so, the input/output voltage ratio can be obtained through,

$$V_{in}(DT_s) = (V_o - V_{in})(1 - D)T_s \tag{3.2}$$

Resulting,

$$\frac{V_o}{V_{in}} = \frac{1}{1 - D} \qquad (V_o > V_{in}) \tag{3.3}$$

But when charging capacitors there is no resistance in the load. The load is fully capacitive and the converter will not work in steady state. Without the resistive component in the output, the system will not reach a balance and the capacitor voltage will rise indefinitely. For this application the boost converter has to be disabled (transistor always “off”) when the desired voltage is reached, stopping the charging cycles. But other conclusions can be retrieved from the analysis of CCM that will be true for our application, like the ripple in the inductor current, equation (*3.4*) represents how much the inductor current rises or falls during its operating states.

$$\Delta i_L = \frac{1}{L} V_{in} \underbrace{(DT_s)}_{t_{on}} = \frac{1}{L}(V_o - V_{in}) \underbrace{(1 - D)T_s}_{t_{off}} \tag{3.4}$$

Opposite to the CCM, the converter can also work in discontinuous conduction mode (DCM), this mode has an additional state where the transistor is “off” but there is no more current in the inductor to be transferred to the output, which for this application can be summarized as a less time-efficient working

mode because it works the same way but there is some time when neither energy is being drawn from the source neither it is being transferred.

3.1.2 Implementation

As stated before, the new kicker system was derived from an existing version, which contemplated a boost converter like the one described in 3.1.1, with a duty cycle of 50% at $32kHz$. From the experience with that converter, problems were identified. The converter was not efficient, most of the time the converter will operate in DCM if the duty cycle is 50%. From equation (*3.1*), it can be seen that the current variation ($\frac{di_L}{dt}$) varies with the inductor voltage (V_L), thus, once the capacitor voltage reaches $24V$, the inductor voltage (V_L) will be $12V$ when charging and -$12V$ during discharge. From the $24V$ to the $95V$ the converter would be in DCM operation.

The solution seemed to be the use of a higher duty cycle but that would create a high current while the capacitors had voltages lower than $24V$, because during CCM, the remaining current from one cycle will be added to the next.

Both problems are visible in the simulations generated in Powersim software "PSIM" [17], also it can be seen that even with 50% duty cycle there is already too much stress on the components because of the initial current that stays above $10A$ for almost $250ms$.

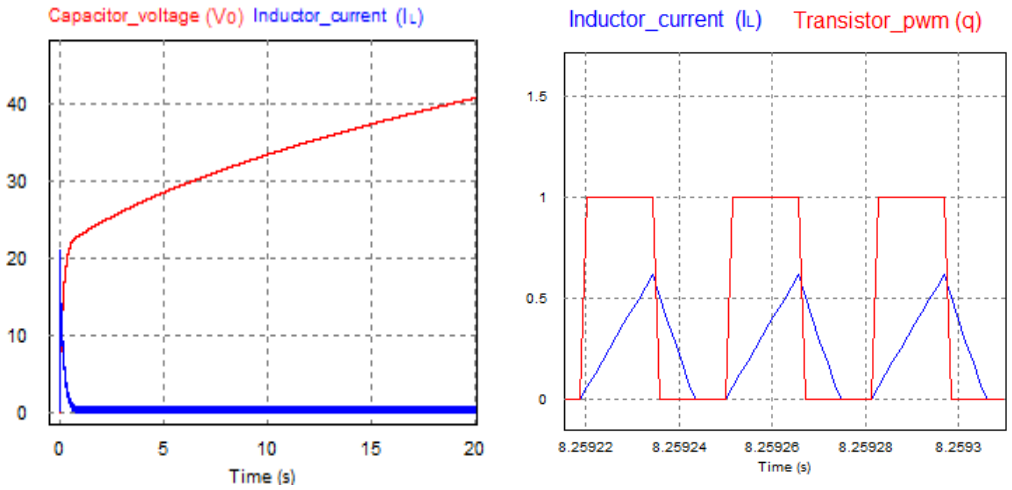

Figure 3.5 - Boost converter running at 32 kHz with 50% duty cycle

To tackle this situation a different control was applied to the basic boost converter. This change results in the current-mode boost converter. This converter consists in the same boost converter but does not have a fixed duty cycle, and instead, the fixed value is the maximum inductor current (i_L). To implement this, the control signal at the transistor gate will have a duty cycle of 99% (ideally 100%), and when the inductor current (i_L) reaches the maximum value, the transistor is turned "off" and the energy is transferred during the rest of the period. The transistor is clocked "turn on". This results in a variable duty cycle that has a maximum "off" time equal to the period of the control signal.

A current mode boost converter was designed and simulated to verify its viability. The schematics for the simulation can be seen in Figure 3.6.

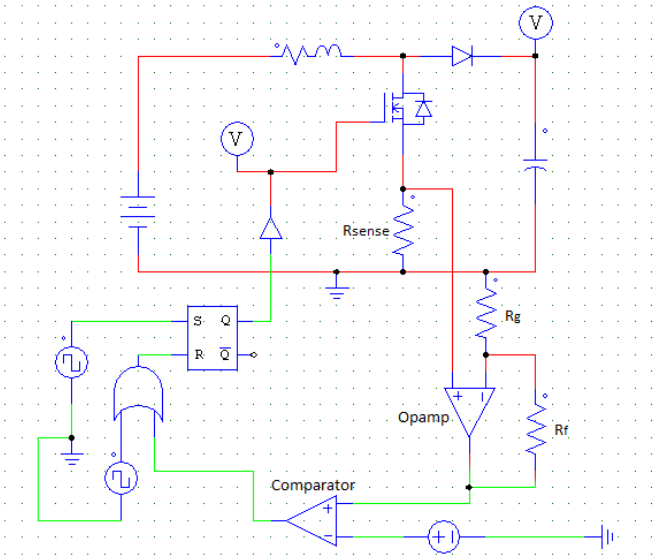

Figure 3.6 - Simulation schematic for a current mode boost converter

To the basic boost converter a very small resistor (0.1Ω) was added in series with the transistor, with the purpose of current sensing. The voltage from the current sense resistor will be low so it has to be amplified with an op-amp with negative feedback (non inverting amplifier [18]). The gain equation for the non inverting amplifier is

$$V_{out} = V_{+} \times (1 + \frac{R_f}{R_g}) \tag{3.5}$$

Besides this, the only difference from the basic boost is the control signal that is fed to the power transistor. For simulation purposes, a set-reset flip-flop is used to create the desired control signal.

The output of the amplifier is submitted to a comparator of which the resulting output will dictate if the inductor current is below or above the desired value. By connecting this binary output through an "OR" logic gate connected to the set-reset flip-flop, the power transistor can be fed with a chosen duty cycle (99%) and frequency ($80kHz$), and will take a low value for the rest of the cycle each time the inductor current reaches the desired maximum value. Figure 3.7 shows the result of the simulation for a maximum current of $3A$.

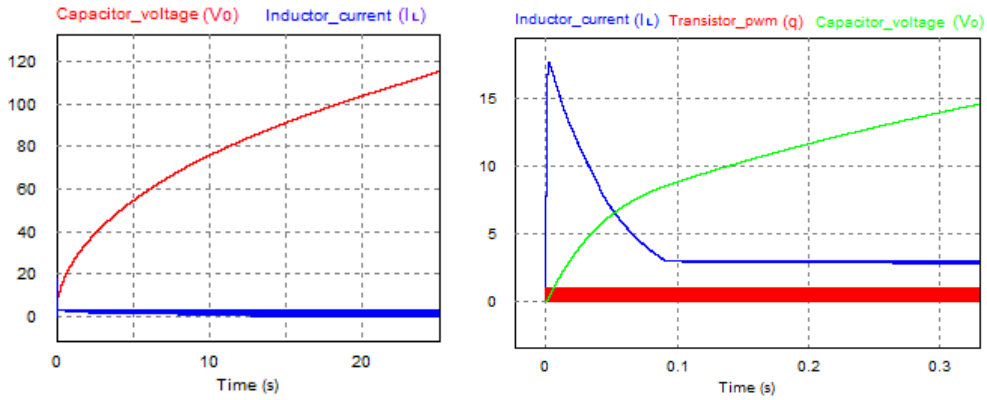

Figure 3.7 - Current-Mode Boost converter simulation results

The results from Figure 3.7 show a faster charging time, with a charging rate much more constant (the boost operates always in CCM). The inductor current was controlled below the $3A$ during the whole charging process but for a very small period when the capacitor voltage is below the input voltage source ($12V$). While the capacitors are under $12V$, the diode is forward-biased by the battery voltage and the capacitor is being charged directly by the batteries. The circuit is unable to control that current, although it was concluded that this spike of current would not damage the circuit and need not to be eliminated as it happens only when the robot is turned on. During game situations the capacitors only go as low as $20V$ and these spikes will not occur. Figure 3.8, is a close up of the converter cycles, where the transistor control signal and the current waveforms can be seen.

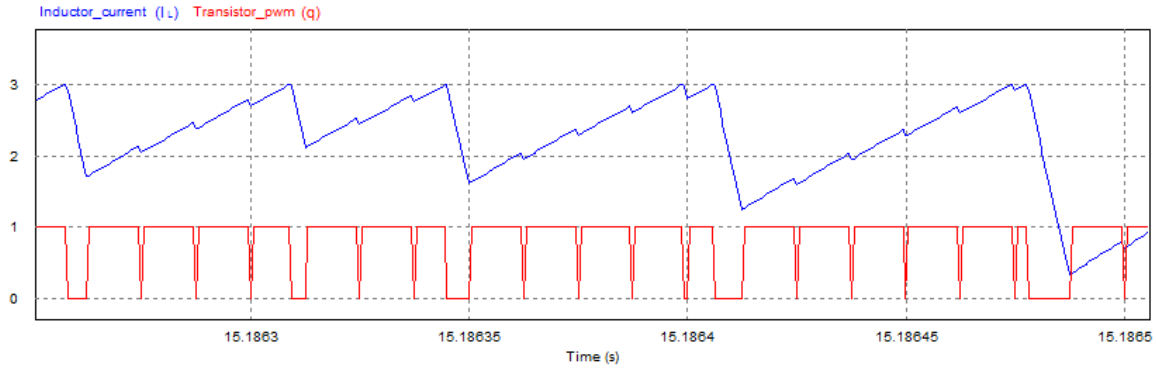

Figure 3.8 - Close up of Current-Mode Boost Converter

This current waveform from Figure 3.8 occurs when the capacitors voltage is close to $90V$ and the discharge of the boost inductor is faster. The circuit only controls the maximum current and then the control signal is low for the rest of the period. The waveform will be irregular as the maximum current can be reached at the beginning or at the end of a period, the simulation shows that when this current limit is reached in the beginning of a period the converter almost enters DCM, this will happen randomly and very few cycles would actually let the inductor current become zero. To completely vanish this possibility, a higher frequency or higher maximum current could be used.

The simulated converter had successful results and a prototype was built.

As Figure 3.2 shows the current-mode boost converter will be separated in two boards:

The “ControlBoard” comprises the circuit that provides the control signal for the power transistor and the capacitor voltage sensor.

To generate a proper control signal for the transistor, a dedicated integrated circuit (IC) was selected. The UCC3803, from Texas Instruments, is a current-mode PWM generator, commonly used in current-mode DC-DC power supplies. The “ControlBoard” schematic is represented in Figure 3.9, where the green wires are connected to the Arduino microcontroller and the magenta wires connect to the “Boost PowerBoard”. The red and black wires represent Vcc and ground respectively.

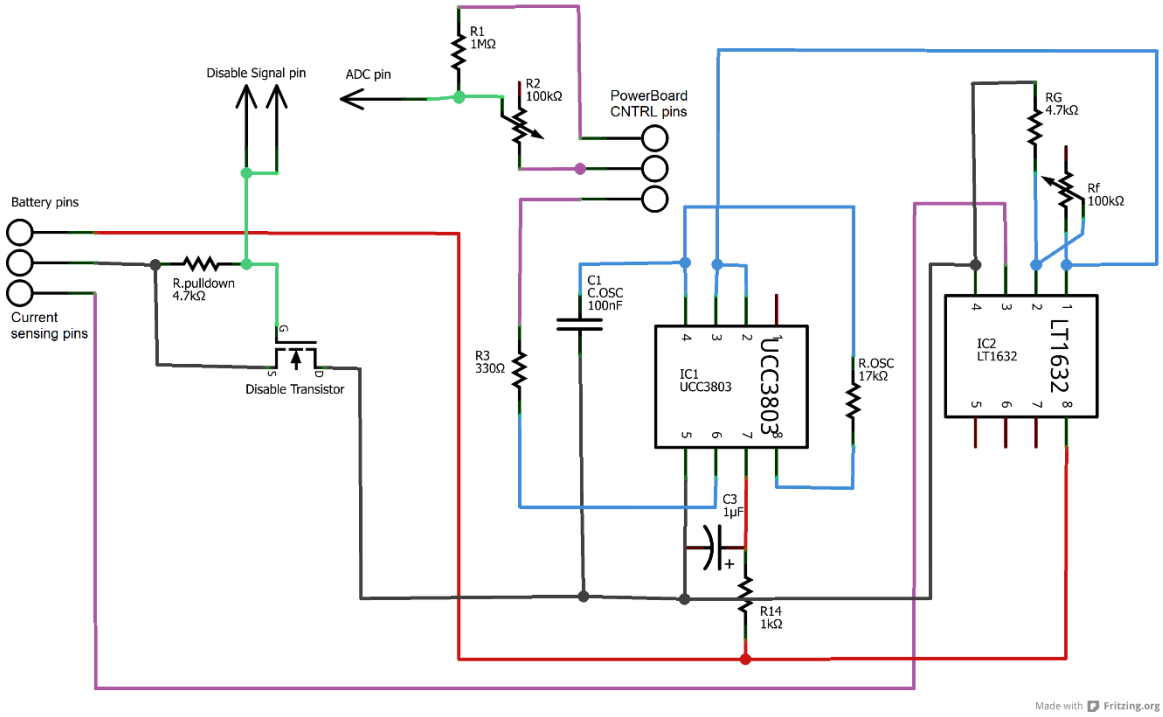

Figure 3.9 - New control board schematic

The LT1632, from Linear Technology, is a dual rail-to-rail input precision op-amp that is amplifying the voltage from a current sensing resistor. With the use of a potentiometer as the “Rf” resistor, it is possible to regulate the maximum current allowed in the circuit. The pin 1(OUT) of the op-amp is connected to pin 3 (CS), from the UCC3803.

The UCC3803 IC will generate the current dependent control signal for the power transistor. The UCC3803 pin 6 (OUT) is a PWM signal with nearly 100% duty cycle. This signal will go low until the end of a period each time the pin 3 (CS) reaches 1 volt. Pins 8 and 4 (REF and RC) are used to control the operating frequency of the control signal. By changing the resistor R.OSC and the capacitor C.OSC, the control frequency can be changed.

The voltage divider, reduces the 100V from the capacitors to be read by the microcontroller analog to digital converters (ADC), and also has a potentiometer to calibrate the values.

With the help of Fritzing [19] software, the layout of the board was optimized.

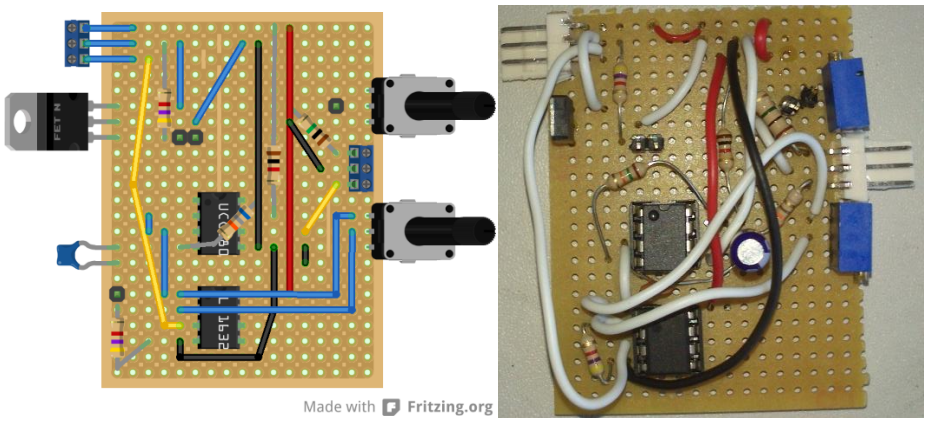

Figure 3.10 - New control board layout and prototype

The “Boost Power Board” was reutilized from the older kicker and has the boost circuit and the current sensing resistor (RSENSE). The CNTRL terminals are connected to the “ControlBoard”.

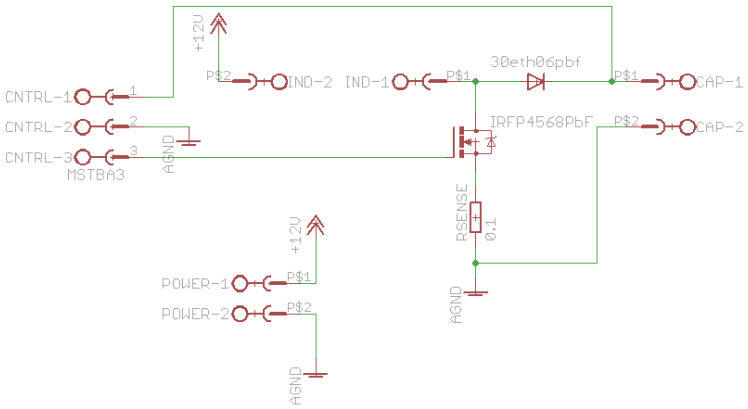

Figure 3.11 - "Boost PowerBoard" Schematic

The gate of the power transistor needs two resistors: A small resistor (330Ω) in series with the gate to reduce the ringing due to the capacitance and inductance from the gate/traces. And a higher resistor ($10k\Omega$) connecting the gate to ground working as a pull-down.

The boost inductor was selected from a handful of handmade inductors varying the number of turns and designs, as a first indicator for the inductor characteristics there must be a trade-off between the resistance and inductance, as both will rise with the number of spires but the lowest possible resistance is desired. The inductor current ripple frequency should also be above $20kHz$ to be above the audible for the human hearing. According to equation (*3.4*) the maximum current variation during discharge for an inductor with $300\mu H$ and control frequency of $100kHz$, is $\Delta i_L = \frac{1}{300\mu H}(95V - 12V)(1 - 0)\frac{1}{100kHz} = 2.7A$. This suggests that using a maximum current above $2.7A$ combined with control frequencies higher than $100kHz$ is enough for the boost to work in CCM during the whole charging process. This correlates with what was observed in Figure 3.8.

The final inductor has 40 turns around an EE shape ferrite core with $1mm$ of air gap and was analyzed in a precision impedance analyzer (Agilent 4294A), which indicated an inductor with $540m\Omega$ and $311\mu H$ at the operating frequency of $32kHz$ (the same values that were used for the simulations).

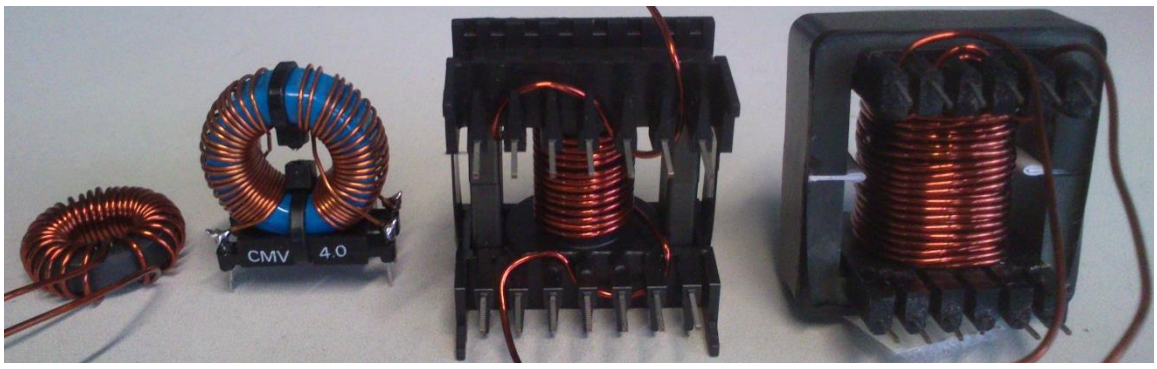

Figure 3.12 - Prototype inductors tested in the boost converter

Finally, a support containing all the kicker electronics, with the exception of the solenoid, was assembled together and installed inside the robot.

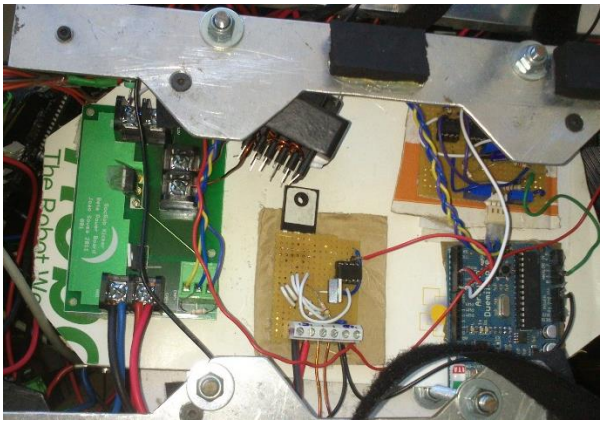

Figure 3.13 - Support with kicker boards

For safety reasons, two voltage sensors should be used to ensure that the voltage from the capacitor is being read correctly, also, a Zener diode with a breakdown voltage of $100V$ combined with a voltage divider could be put in parallel with the capacitor and connected to the microcontroller, so in a fault situation, if the capacitor reaches $100V$, the microcontroller port would be triggered, and shutdown procedures could be activated.

3.1.3 Results

The control board was tested and the control frequency and the maximum current were adjusted to optimize the performance. Because of being clocked “turn on”, the higher the frequency the better, as long as other components keep up. The same is true for the maximum current. Increasing any of them will result in faster charging speeds due to the higher average current in the circuit. Two waveforms are shown in Figure 3.14, where the inductor current (I_L) sensed by a commercial current probe (Tektronix A6302 paired with the current probe amplifier Tektronix TM502A) is represented as yellow, the magenta waveform is the (current sensing) voltage at the output (pin 1) of the amplifier, and finally the cyan waveform is the control signal at the gate of the power transistor (CNRTL3).

Figure 3.14 on the left, combined $2.6A$ as maximum current with a control frequency of about $40kHz$. The result was a periodic behavior because the converter worked always in DCM.

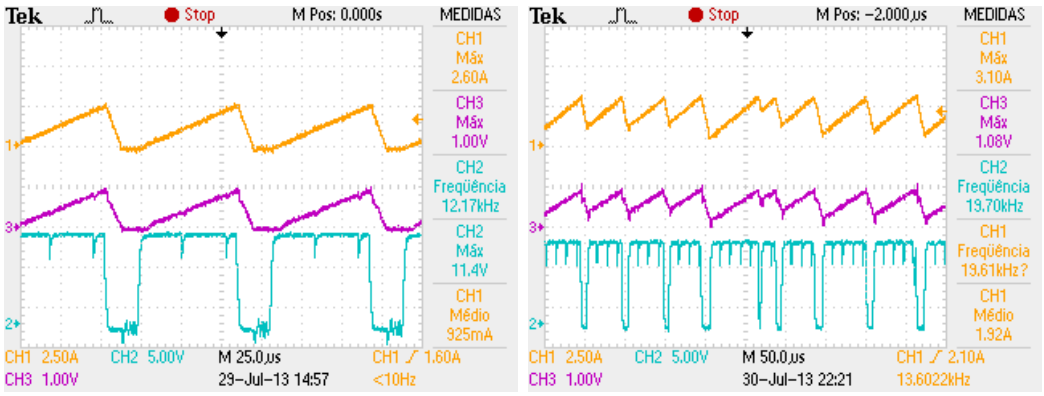

Figure 3.14 - Laboratorial results of the current-mode boost converter

The figure on the right combined a frequency of nearly 80kHz and a maximum current of 3.1A. With this combination the converter worked in CCM which can be verified by the waveforms.

Also, the tests show that the current sensing resistor and the amplifier readings are accurate just like the commercial current probe. The oscilloscope frequency readings are incorrect due to non periodic behavior of the waveforms.

The time of charging was measured with different values of current and frequency and the results are shown in Table 3.1 and Table 3.2. The charging time represents a full charge from 12V to 95V and the recharge time is the charge from the voltage after a full power kick (around 70V).

Table 3.1 - Capacitor charging times at 120kHz changing the max current

Max. Current [A]	Charging time [s]	Recharging time [s]
1.2	42	21
1.8	26.5	12
2.5	18	8
3.2	12	5
5	8	4

Table 3.2 - Capacitor charging times at 2.5A, changing the frequency

Frequency [kHz]	Charging time [s]	Recharging time [s]
25	26	14
32	24	10
48	22	10
64	20	10
100	18	9
120	17	8
147	17	8

The combination of using a control frequency of 120kHz with the maximum current of 3.2A, took 12 seconds to completely charge the capacitors and was chosen to be used in the robots. From the results it is visible that there's not much to gain from further stressing the circuits, especially taking into account that being able to repeat a kick every 5 seconds is less than what is supposed to happen in the game.

In case of two sequential kicks, the energy left in the capacitors after one kick is still enough to produce a good shot (with less power). The waveforms from the boost in its final configuration are shown Figure 3.15.

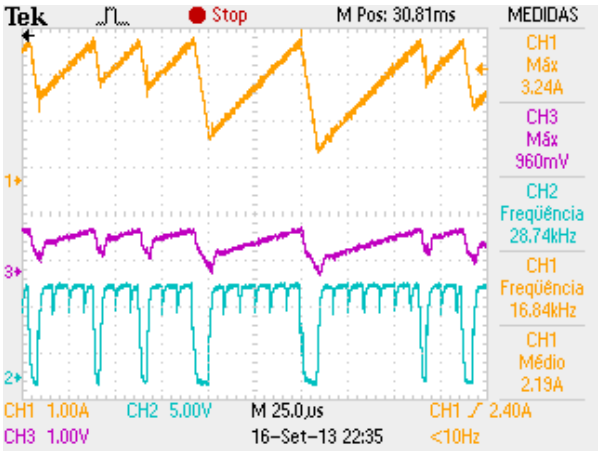

Figure 3.15 - Boost waveforms with 3.2A of maximum current and 120 kHz of control frequency

The average current drawn from the batteries is around 2.19A, which is under the batteries limits and still leaves room for the other electronics in the robot, like motors and camera.

From the time the boost takes to completely charge the capacitors with is maximum energy, the average output power of the converter can be estimated. With equation (*3.12*), $W = \frac{1}{2}95^2 \times 0.088 = 390\text{J}$, and the time of charging is 12 seconds, so the average power must be around 32.5W.

Figure 3.16, shows the voltage waveform of the capacitor (Vo), when charging, kicking, recharging, and safely discharging the capacitors to turn off the robots.

The discharge procedure is shown as the big vertical line going from 70V to 20V, this is not the correct waveform of the discharge because the discharge is slower. The reason is that during the discharge procedure, the voltage readings are only being monitored by the microcontroller and were not registered in this waveform. The discharge procedure is explained in 3.2.3

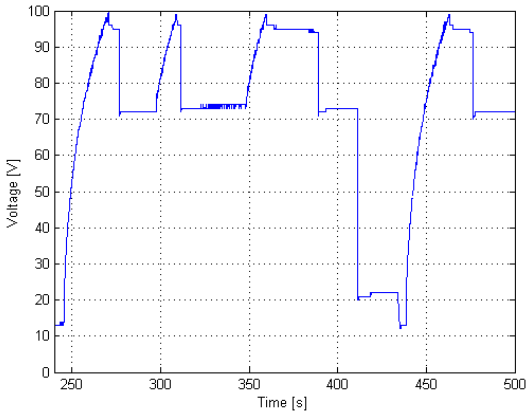

Figure 3.16 - Charging the capacitor at 120kHz and 1.8A

3.2 Electromagnetic actuator

The energy charging subsystem was described in the previous section. The solenoid and the board to discharge the capacitors onto the solenoid are explained in this section.

The electromagnetic actuator is the part responsible for converting electric energy into the linear movement to kick the ball.

3.2.1 Theory

There are two types of linear electromagnetic actuators that can be built using solenoids.

In the **inductance actuator** the rod is made of permanent magnets or has diamagnetic properties. This way the rod can be repelled by the change of the magnetic field. Usually the solenoid is composed of multiple coils, giving the ability to control the magnetic field of the stator along the length of the actuator. Then, combined with the ability of measuring the precise position of the thrust rod, the pulse currents in the coils are synchronized to maximize the thrust. The example in Figure 3.17 uses permanent magnets inside the rod and hall sensors for position feedback.

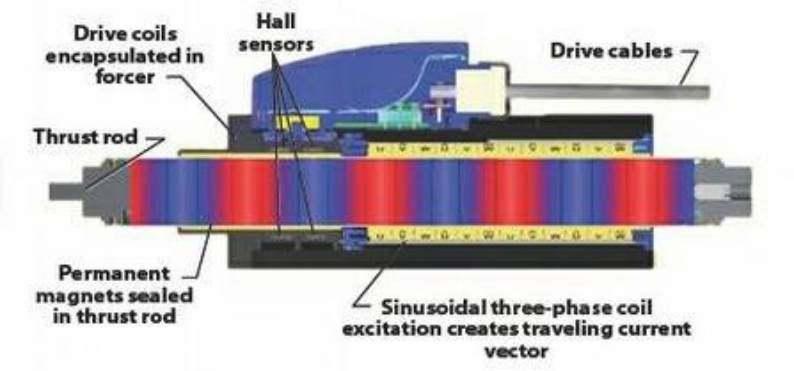

Figure 3.17 - Cross section of an inductance actuator [20]

The **reluctance actuator** is the one that will be further explained in this section and requires only the solenoid and the ferromagnetic projectile (rod) to work. The magnetic field created by the solenoid creates two separate magnets, one inside the coil and another in the rod, both with the same orientation, thus the rod sees an opposing pole and is attracted to it.

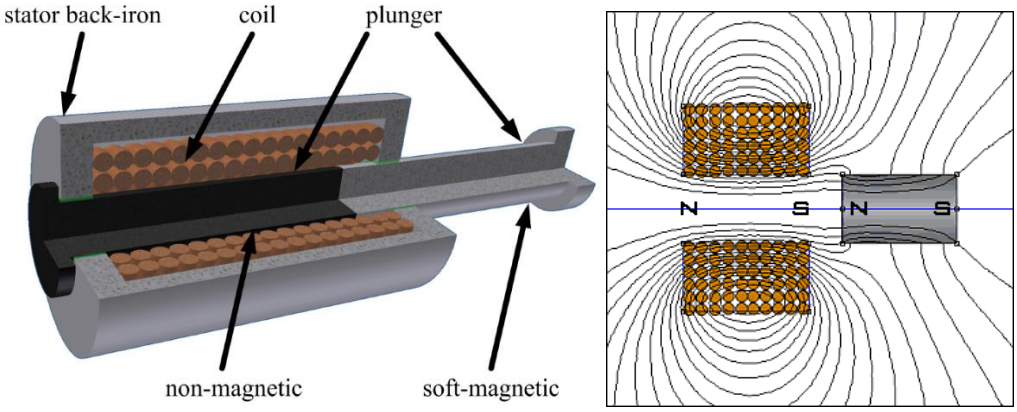

Figure 3.18 - Basic principles of a reluctance actuator [8] [15]

When a current pulse is applied to the solenoid, the magnetic force acts to move the projectile in the direction of decreasing magnetic reluctance, which is the resistance to the magnetic field and is inversely proportional to the magnetic permeability (μ). The total reluctance of the solenoid is given by the sum of the reluctances in the path of the magnetic flux (B).

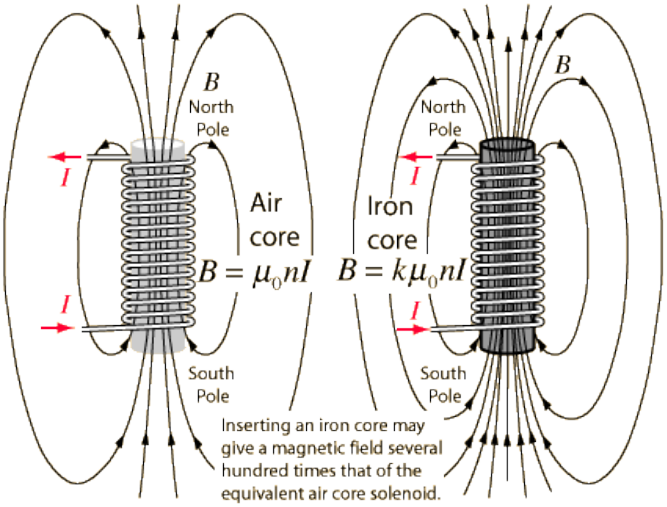

Figure 3.19 - Magnetic flux lines in solenoids [21]

Thus, if the core of the solenoid becomes ferromagnetic (as in the rod material), the global magnetic reluctance will be lower because of the higher permeability of the path, thus the projectile will always be attracted to the middle of the coil. The magnetic force depends on the core itself and the flux linkage (λ) created by the solenoid, which depends on the inductance of the coil (L) and the current (I).

$$\lambda = \mathrm{LI} \tag{3.6}$$

Hence, the coil inductance [16] can be given by,

$$L = \frac{\overbrace{\overbrace{\overbrace{\left(\frac{NI}{l}\right)}^{H}\mu}^{B}\,A\,N}^{\Phi}}{I} = \frac{\lambda}{I} = \frac{N^2}{\frac{l}{\mu A}} = \frac{N^2}{\Re} \tag{3.7}$$

Where, the magnetic field, $\mathrm{H} = \frac{NI}{l}$, N being the number of turns, I is the current and l is the length of the solenoid. The magnetic flux density, $B = H \times \mu$, where μ is the magnetic permeability. The magnetic flux, $\Phi = B \times A$, where A is the section of the solenoid. Finally, $\Re$ is the magnetic reluctance.

From equation (*3.7*) it can be seen that the inductance depends on many factors. Also some of these factors have an influence in the current running in the coil as is the case of the number of spires and area of the spire. Increasing these values will increase the length of the coil wire, increasing its total resistance, thus reducing the current in the coil wire.

For the actuator to be effective, all of these factors have to be well-balanced and this can only be achieved through simulation and experimentation, but there is one factor that does not interfere with the maximum current: the permeability of the magnetic path. The interior of the solenoid cannot be modified

because it's the path for the thrust rod, but the outside can be covered with ferromagnetic material to reduce the total reluctance of the magnetic path.

$$\Re_{total} = \Re_{gap} + \Re_{shell} = \frac{l_{gap}}{\mu_{gap} A_{gap}} + \frac{l_{shell}}{\mu_{shell} A_{shell}} \tag{3.8}$$

This shell will also be useful to prevent the propagation of magnetic noise to the robot.

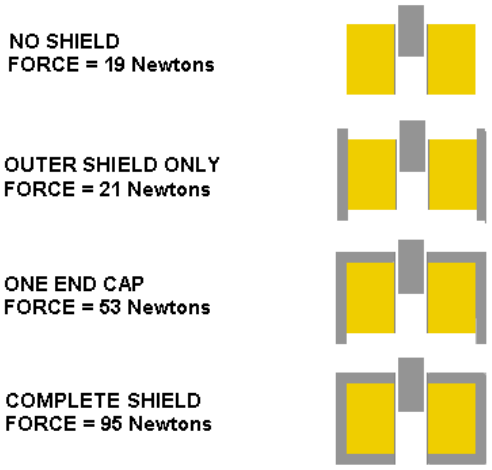

Figure 3.20 - Effect on the coil's force due to magnetic shielding [22]

Finally there are other characteristics of the solenoid that will have an impact in its design. Given the high inductance of the solenoid, it is difficult to rapidly change current through the circuit. The current growth can be expressed as,

$$I = \frac{V_L}{R}\left(1 - e^{-(R/L)t}\right) \tag{3.9}$$

From which a time constant (τ) can be extracted,

$$\tau = \frac{L}{R} \tag{3.10}$$

At time $t = \tau$, the current reaches 63% of its final value, in 2τ, 86% and so on, the characteristic curve of current for a solenoid is shown in Figure 3.21.

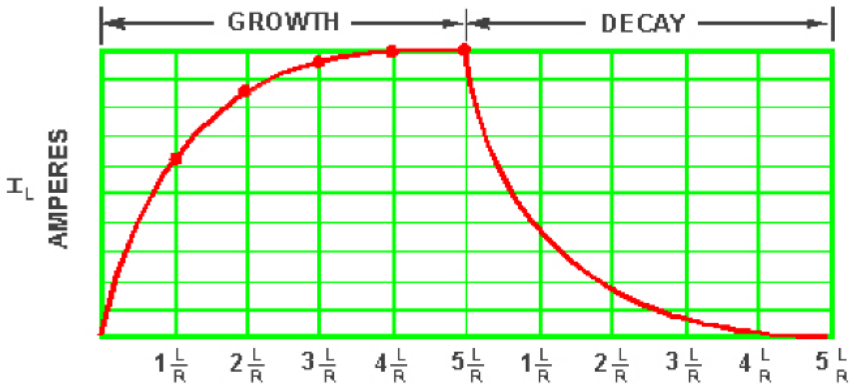

Figure 3.21 - Current growth and decay, in inductors [23]

There is also another time to take into account: given that the robot dimensions will limit the size of the solenoid, and force will only be applied until the rod reaches the middle of the solenoid. For the final speed to be achieved, the acceleration must be very high, given the reduced length available for acceleration. Assuming the acceleration (a) is constant, and knowing the length available for acceleration (x_f) and the final speed desired (v_f), the acceleration time (t_f), the classic equations for linear movement give an estimation of the amount of time where force is favorable.

$$x_f = \frac{1}{2} a {t_f}^2 \; ; \; v_f = a t_f ; \quad \rightarrow \quad t_f = \frac{2x_f}{v_f} \tag{3.11}$$

Where, t_f is the time where force is favorable, x_f is the length available for acceleration, and v_f is the final speed desired.

The actuator would not work without the power source. The capacitors and their voltage have a strong influence in the maximum current of the solenoid, but the capacitors need, not only voltage but also capacitance. The amount of energy stored in a capacitor is given by,

$$W = \frac{1}{2} V^2 C \tag{3.12}$$

Where, V is the voltage and C is the capacitance.

The capacitor must have a high voltage to be able to generate the high current needed to create the magnetic field, and the capacitor energy must be much higher than the energy that needs to be transmitted to the ball. There will be big losses converting the electric energy into kinetic energy in the rod, and losses transmitting the kinetic energy from the rod to the ball.

The kinetic energy is given by,

$$W = \frac{1}{2} m v^2 \tag{3.13}$$

Where, m is the mass and v is the velocity.

3.2.2 Implementation

The starting point to develop the solenoid for SocRob, was an older solenoid that was designed and built as part of another MSc Thesis [24].

Once the DC/DC converter from section 3.1 was built, the “kickboard” was developed so the older solenoid could be used. Figure 3.2 describes the actuator architecture.

3.2.2.1 KickBoard

The “KickBoard” only takes care of controlling the discharge of the capacitors through the solenoid, but caution is needed because of the high current that will flow through the components.

The former relay used in the original kicker was discarded due to its high switching time that was not reliable to choose different pulse (kick) times. Instead, a power MOSFET transistor capable of sustaining the high current expected, was used. The gate of this transistor also has a pull-down resistor (for safety).

The board also features a diode to let the current from the solenoid dissipate (freewheel) when the circuit is opened, and an optocoupler to receive the kick signal from the microcontroller and drive the transistor gate with $12V$. Because of the high current expected (even if only for $50ms$) the strip board is not a good option, so to prevent damages, two strips were used per pin to distribute the current and dissipate heat. A proper printed circuit board (PCB) should be done in the future. The schematics and layout of the prototype boards are shown in Figure 3.22 and Figure 3.23.

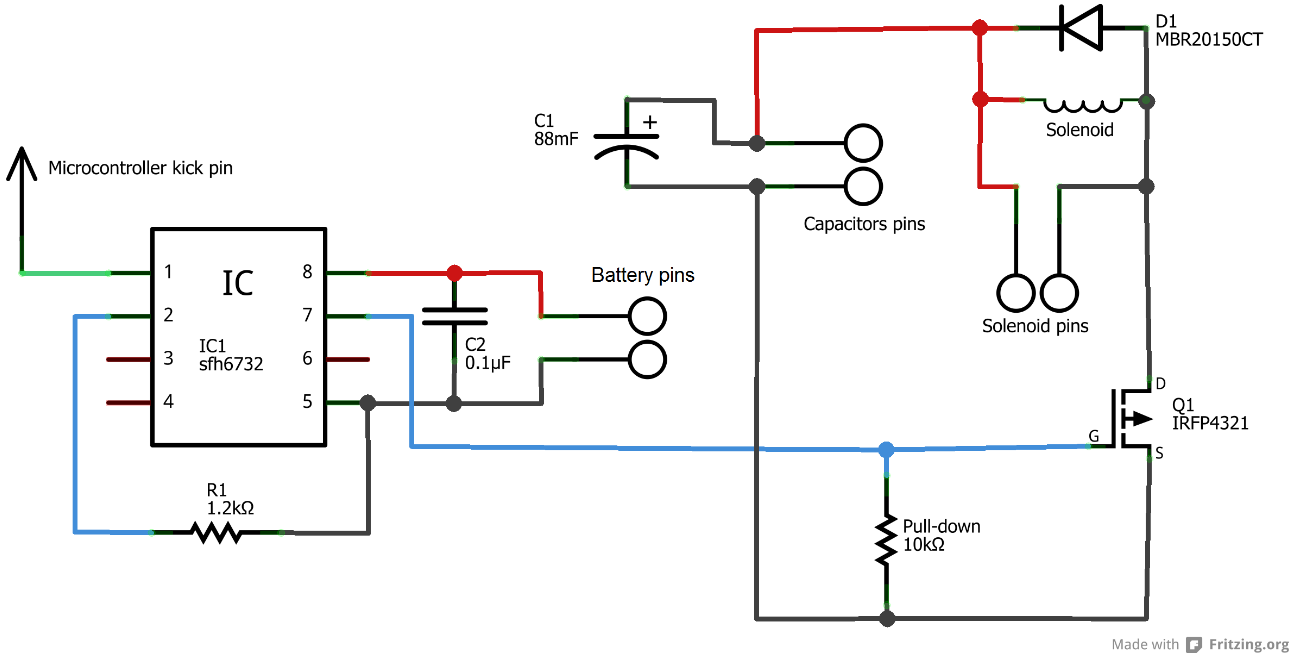

Figure 3.22 - Kickboard schematic

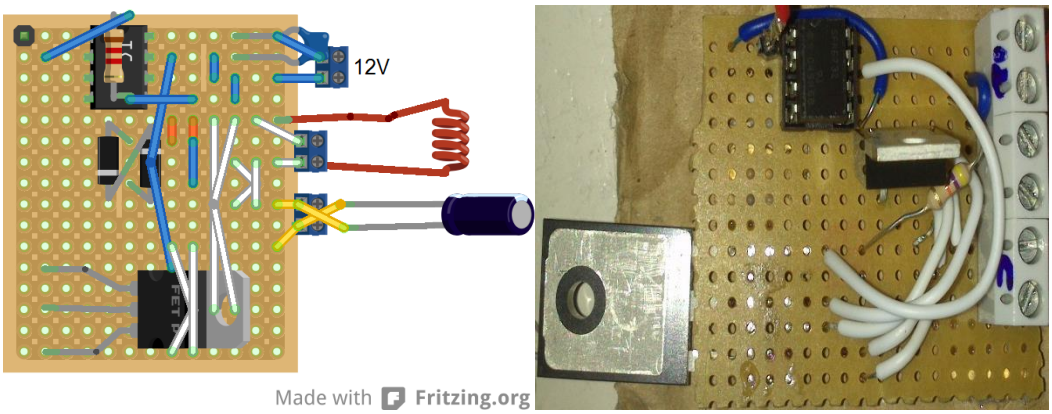

Figure 3.23 - New kickboard layout and prototype

3.2.2.2 Solenoid

With the completed prototypes of the “KickBoard” and the power converter, the original solenoid was tested with the capacitors charged at maximum voltage, something that wasn’t possible with the older circuit. The solenoid was able to do decent shots but was still away from the desired quality. Results from the tests carried with the original solenoid are shown in section 3.2.3.

Table 3.3 summarizes the characteristics of the capacitors and the original solenoid that was experimentally tested.

Table 3.3 - Capacitor and Solenoid parameters

Parameter	**Value**
Voltage $[V]$	95
Capacitor $[mF]$	88
Coil Inductance $[mH]$	2.58
Coil resistance $[m\Omega]$	1.53
Coil max current $[A]$*	62
Coil wire diameter $[mm]$	1
Coil turns	440
Coil length $[mm]$	130
Tube inner diameter $[mm]$	32
Tube outer diameter $[mm]$	42
Rod diameter $[mm]$	28
Rod length $[mm]$	100
Total rod weight $[g]$	0.7

* The coil max current was calculated based on Ohm's law.

To find a better candidate it is not feasible to build different solenoids and test them until a better one is found.

Simulations of the solenoid magnetic properties were done with the help of the Finite Element Method Magnetics (FEMM) [25] software. Through multiple simulations, the influence of the solenoid parameters in the performance of kicking the ball, can be studied.

First the geometry of the problem had to be drawn, the program is capable of axisymmetric simulation and so, the representation of the solenoid and rod were drawn with the real dimensions from the original solenoid.

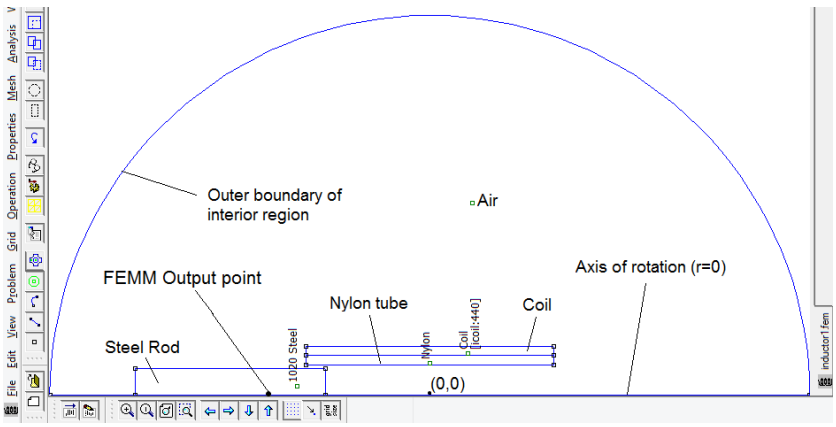

Figure 3.24 - FEMM representation of the solenoid/rod

Figure 3.24 represents a cross section from the longitudinal axis of the solenoid to the outside. The solenoid becomes clear if all the lines make a revolution around the axis of rotation. The program has a library of materials from which the closest to our case were chosen.

The number of turns in the coil is a mere sum of currents, the program works with the current density in the whole area of copper. The program doesn't model everything, the current must be set manually and won't be affected by the copper resistance, there's no way to simulate the discharge of the capacitors exactly as our circuit will work, but using a fixed current as the one expected when discharging $85V$, should be a good compromise with the actual situation, because the capacitors will discharge from $95V$ to $70V$ during one shot.

Starting from this, a deep magnetic simulation can be performed, and the software features script-like commands with MATLAB integration, to ease the modification of parameters and process iterative simulation.

Figure 3.25 represent the magnetic simulation using the original solenoid with 440 turns of wire and a current of $58.7A$. The figure in the left has the rod at the entrance of the solenoid (starting position), and shows the magnetic flux lines. The figure in the right has the rod at $65mm$ from the middle of the solenoid (position where the force is stronger), and do not show the magnetic flux lines for better visibility of the color patterns representing the magnetic flux density (B).

Both simulations show the FEMM output with detailed information (with especial attention for the magnetic flux density $|B|$), calculated for a specific point of the rod (shown in Figure 3.24).

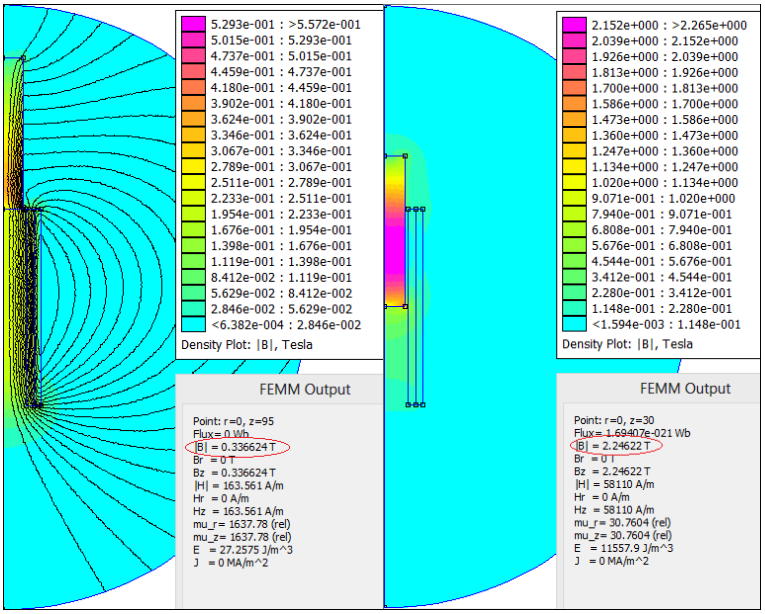

Figure 3.25 - FEMM magnetic simulations

In the simulations shown in Figure 3.25, it can be seen that during the trajectory of the steel rod, the magnetic flux densities (B) change. In the image on the right, the magnetic field created by the solenoid is enough to create magnetic flux densities around $2.25T$. By comparison of these values and the B-H curve of the steel, it can be seen that the steel rod is actually reaching saturation values.

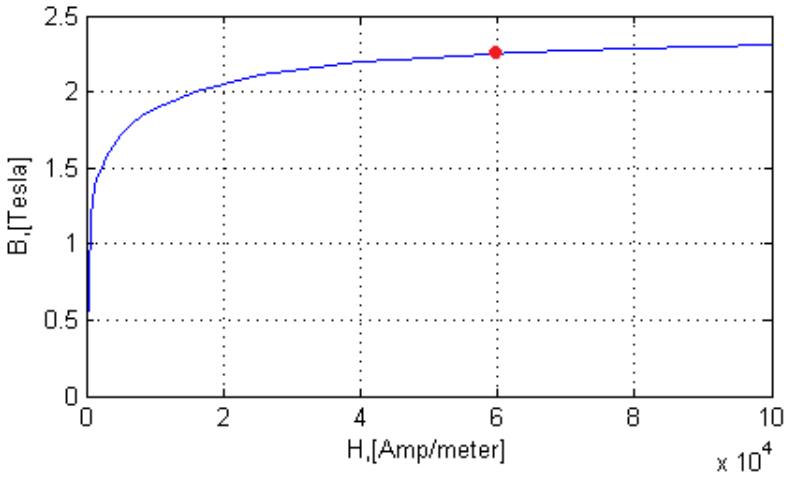

Figure 3.26 - B-H curve for 1020Steel

To study how to maximize the performance, MATLAB scripts were written to calculate the forces applied in the rod at different positions and varying dimensions. The software can calculate many physical quantities, one of which is the "z part of steady-state weighted stress tensor force", this is used in the coil-gun example [26], made by the author of the program, to compute the magnetic force felt by the rod.

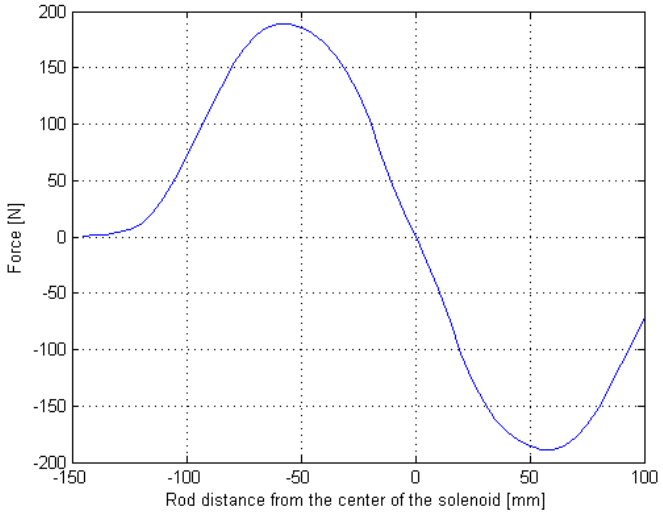

Figure 3.27 - Magnetic force vs. rod position

The simulation presented in Figure 3.27 confirms that force is only positive until the rod reaches the middle of the coil, then current should be cut, letting the rod continue forward with maximum energy.

From the force values, and knowing the total weight of the rod, the final velocity of the rod can be derived with the kinetic energy, equation (*3.13*), and the work-energy principle, which is given by.

$$W = F \times d \tag{3.14}$$

Where, F is the force felt by the rod and d is the distance travelled.

To ease the simulation process the rod was moved $5mm$ at each time and the force was considered constant during that displacement.

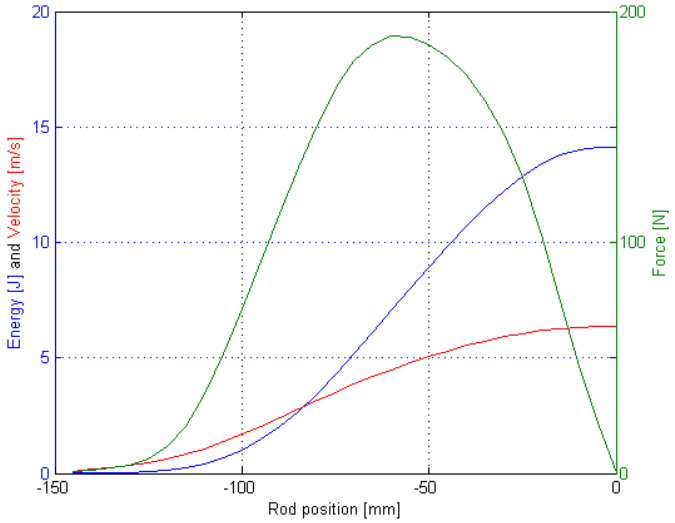

Figure 3.28 - Simulated velocity of a shot

The simulation results give an estimated final velocity of 6.35m/s, which is the expected given the actual performance of the kicker. The test results in 3.2.3 achieved 5.5m/s with about 0.31 m/s of standard deviation. The reasons for the simulation to differ from reality are:

- The steel used from the material library may be a poor match for the steel we are using.
- The simulation uses constant current when it should be dynamic.
- Eddy currents induced by motion are not modulated.
- Friction is not modulated.
- The simulation calculates the kinetic energy of the rod, and the transference of kinetic energy from the rod to the ball has losses.

Several existing works [15] [22] [23], already did a lot of experimentation regarding what is best in terms of solenoid design for their coil guns, and show how most aspects influence the coil-gun. The same rules apply in our case so, there's no need to do those simulations. Only the simulations to see how much improvement can be obtained in our specific case are shown in this thesis.

According to the these sources and our solenoid model, the parameters that had room for improvement were simulated to check the individual improvement, and then, a simulation with all of the improvements together is performed to measure the total gain in rod velocity. Those parameters are:

1. Minimize the air gap between the rod and the coil. This will reduce the solenoid section and reduce the length of wire in each turn, thus reducing the solenoid resistance. The nylon tube can have is thickness reduced and the inner radius of the tube could be closer to the core. The gap was reduced from 7mm to 2mm in radius.
2. Minimize the global reluctance of the magnetic path, this is achieved by using a shell of ferromagnetic material around the coil, concentrating the flux lines around the coil. Given that the magnetic permeability of steel is much higher than air, 5mm of shell thickness is enough to conduct most of the flux.

3. Adjust the rod length, the rod length is smaller than the coil and the optimum size for this case is the same as the coil (increase in mass was compensated). It was increased from 100mm to 130mm.
4. Adjust the number of turns in the coil, each turn will add more contributions to the magnetic field but will decrease the current in all turns. This should be incremented until the magnetic flux (B) values in the rod are in the saturation region. When in the saturation region, increasing the number of turns will have a very low contribution, and the increased inductance opposes the variation of current which will have a negative contribution that reduces the performance.
5. Increase the voltage from the capacitors, the higher voltage will generate a higher current in the coil and increase the magnetic field created.

Changes number 1, 2 and 3 were simulated individually and compared to the original solenoid without modifications, Figure 3.29 shows the comparison of the results.

The change number 4 cannot be simulated in FEMM because the program uses a fixed current during the simulations and does not model the influence of the inductance in the current.

At the end, Figure 3.32 shows the simulation results of changing parameter number 5, to check how much voltage would be needed to put the original solenoid with the desired power. This change was not shown with the other simulations because it does not involve changing the solenoid, and was not implemented because of being expensive. The capacitors and power components do not support a higher voltage.

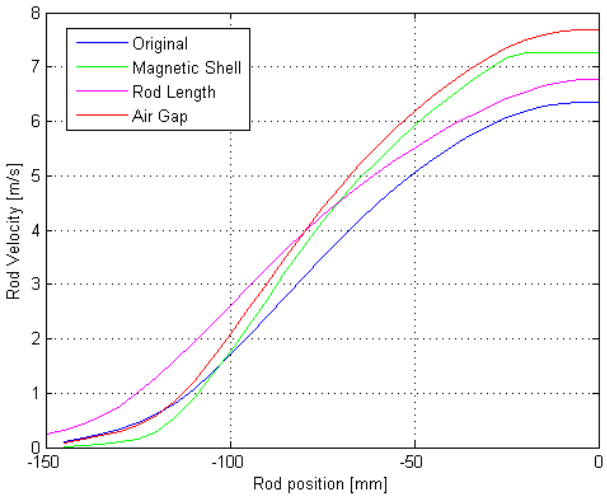

Figure 3.29 - Simulation results for individual improvements

Figure 3.29 shows that each of the changes simulated resulted in improvements in the final velocity of the rod.

The improvement achieved by increasing the length of the rod is good and is larger than it seems because the rod also increased its mass.

The magnetic shell simulation becomes flat near the middle of the rod. This only happens because the rod in the simulation is smaller than the coil, but since the longer rod is more efficient, this will not happen if both changes are made simultaneously.

When all the above improvements are put together the simulation shown in Figure 3.30 predicts a final velocity of $9m/s$, which is close to the desired objective, and possibly enough for the desired application. The script for this simulation can be seen in Appendix A.

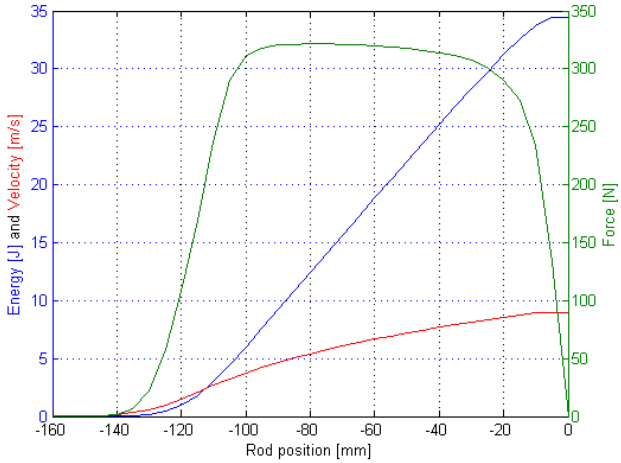

Figure 3.30 - Solenoid simulations with all the improvements

Also it is important to check the saturation levels of the new model. Figure 3.31 shows that the magnetic shell has successfully concentrated the flux lines and the magnetic flux densities are higher, reaching values around $2.5T$.

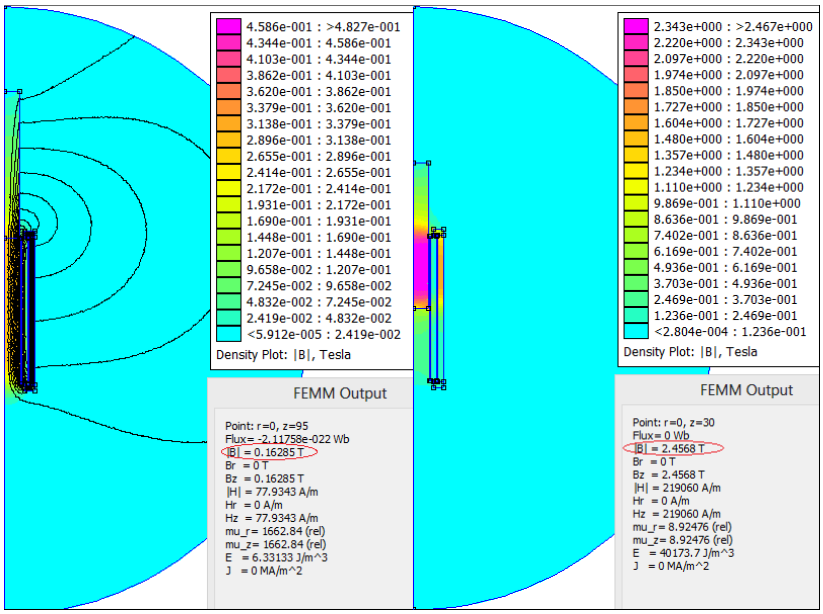

Figure 3.31 - Magnetic Flux Density for the final solenoid model

Finally the simulation changing the capacitors voltage is done. Figure 3.32 shows how much the voltage of the capacitors, influence the rod velocities.

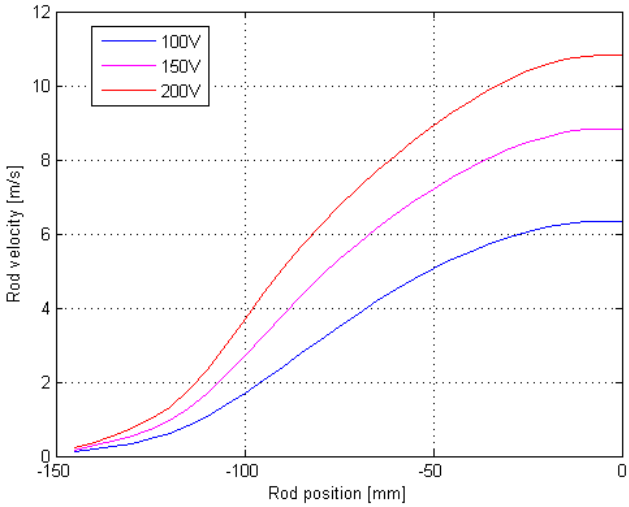

Figure 3.32 - Rod velocity vs. Voltage

The result is that the original solenoid, using 200V as a power source, would be enough to kick the ball at more than 10m/s. This was not the solution sought because it would be expensive and the lower voltage is less dangerous.

The final solenoid/rod design parameters are summarized in Table 3.4.

Table 3.4 - Final solenoid/rod parameters

Parameter	**Value**
Coil inductance [mH]	2.58
Coil resistance [$m\Omega$]*	1.15
Coil max current [A]*	82
Coil wire diameter [mm]	1
Coil turns	440
Coil length [mm]	130
Tube inner diameter [mm]	30
Tube outer diameter [mm]	32
Rod diameter [mm]	29
Rod length [mm]	130
Total rod weight [g]	0.85
Resistance [Ω]	2.34
Max current [A]	40.5
Shell material	Steel
Shell thickness [mm]	5

* Values calculated based on the other parameters.

3.2.2.3 Mechanical designs

To check and help design the new solenoid within the available dimensions, a 3D model of the robot was designed with Autodesk Inventor, focusing on the parts relevant to this thesis. The inside and front part of the robot (space available for kicker and dribbling system) were designed with more detail. The 3D model of the SocRob robot did not exist, and it is expected to be useful in the future for new projects using the SocRob platform, which should update the model if changes are made.

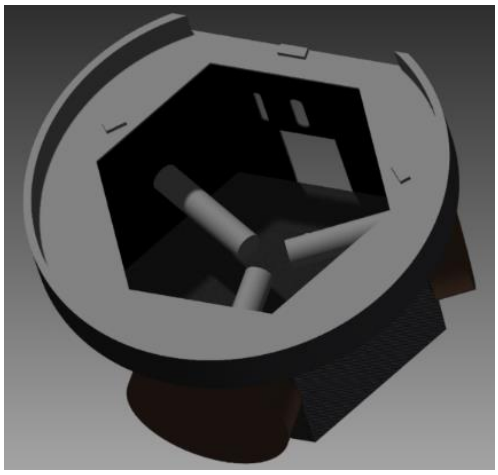

Figure 3.33 - 3D model of SocRob Platform

In this thesis the 3D model will be useful to design the final solenoid and its support to the robot within the space available, as well as the dribbling system in Chapter 4. There is still a difficulty regarding the design of the support for the solenoid, because the robots have holes with different dimensions on the bottom, where the support has to be fixed.

The original solenoid was poorly manufactured. The problems found were:

- The returning of the rod to the start position was carried by rubber bands. This is the easiest way to solve the problem but the complete restitution is not guaranteed unless more force is used, resulting in power losses in the rod.
- The rod was secured inside the robot by a rope. When the robot kicks without hitting anything the strength of the kick damages the rope until it eventually breaks.
- Because of the strength of the shots, the force felt by the turns of copper made them slide along the nylon tube.

In the design of the new solenoid solutions for these problems were tried.

The rod, like the original one is made of two parts. A ferromagnetic part (steel), used in the simulations. And the nylon part that is responsible for maintaining the rod in the coil when fully retracted, and by extending the stroke outside of the robot to hit the ball.

Instead of the strings grabbing the rod, the rod was designed with a wider ring at its back. This ring has to be covered with a softer material like foam or rubber to soften the impacts against the coil tube. Concerning the rubber bands, it was analyzed if it was possible to use an inclination on the solenoid so gravity would take care of returning the rod to its initial position but there was not enough space inside of the robot.

The optimized solenoid and rod were then designed to fit the robot and added to the 3D robot model with appropriate supports.

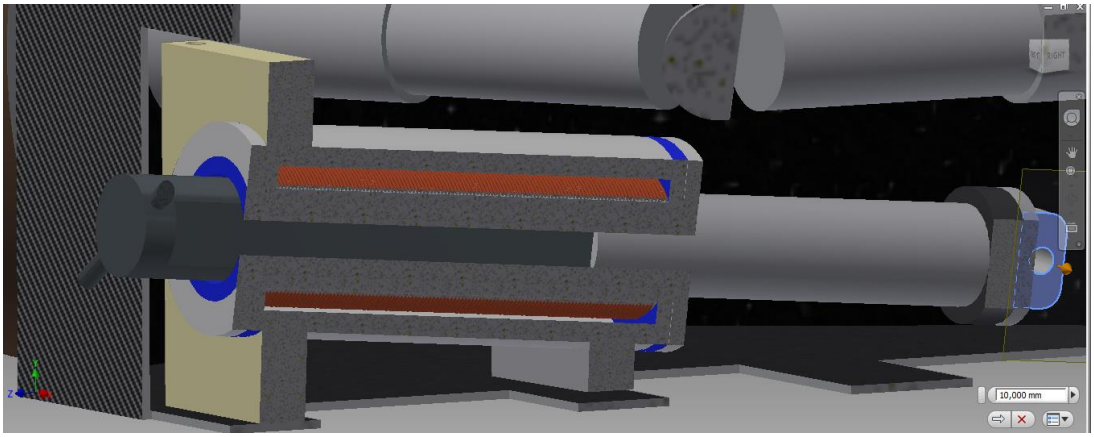

Figure 3.34 - Planar cut view of the solenoid inside the robot

The new model was able to fit inside the robot, but is a little too close from the front of the robot, it may be a problem if the rod hits the ball too soon without gaining speed first.

The magnetic shell was designed by means of a steel tube and two washers to economize material and reduce costs. Detailed designs are shown in Appendix B.

To maximize the ball velocity even further, a mechanism to block/release the rod could be used to bypass the rising slope of the solenoid current. This way the rod would be released with a higher initial acceleration. This was not used given to the restricted space and complexity that the system would add.

3.2.3 Results

The kickboard developed to control the current pulse was tested in the laboratory to check the ability to withstand the current and cut it accurately.

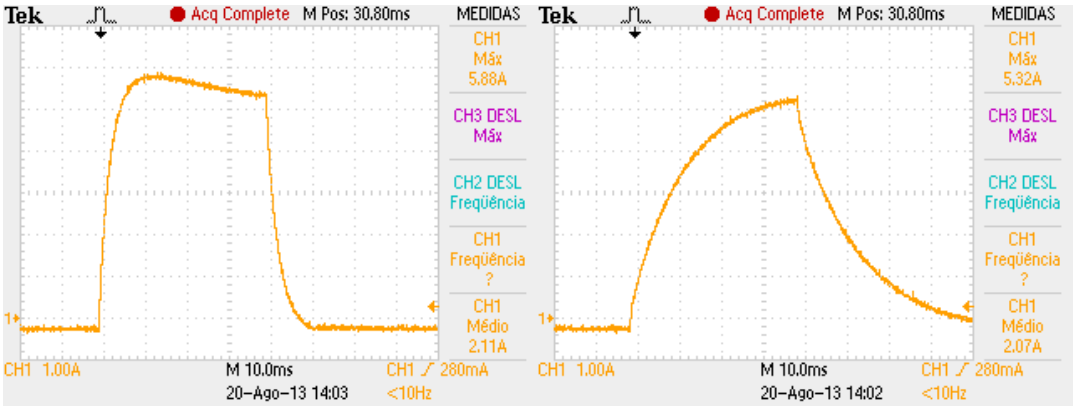

Figure 3.35 - 40ms solenoid current pulse, (left) rod at start position, (right) rod in the middle

These waveforms were taken discharging the capacitor with only $12V$, because the current probe is not able to measure the higher current expected when discharging the $95V$. The yellow line represents the solenoid current and as expected, the waveform changes with the position of the rod because it affects the solenoid inductance. In the left plot, the rod was at the entrance of the solenoid and current takes only a small time to rise which is small compared to the pulse. On the right plot, the rod was in the

middle of the solenoid, in this situation the inductance is higher and current takes much longer to rise or fall. Due to the inductance, when the current is cut off, a considerable amount of current continues flowing through the diode and unwanted forces may be applied to the rod.

Figure 3.35 also shows that the 40ms pulse is accurate.

The kickboard is able to withstand the current pulses needed to shoot the ball, but there's also the need to completely discharge the capacitors to turn the robot off. It would be very dangerous to let the capacitors charged at 95V, and is not safe to do this by kicking several times with the risk of hitting something or someone. A discharge procedure using small pulses that won't have enough strength to move the rod was implemented and tested.

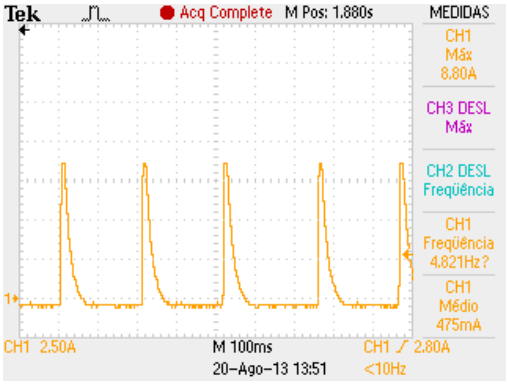

Figure 3.36 - Discharge procedure

Figure 3.36 shows the solenoid current pulses that are triggered when the discharge procedure is called. Each pulse is 7ms wide and has enough time in between for the current to reach zero, the procedure continues until the capacitors reach 20V.

Next step was to test how the whole system behaved kicking soccer balls.

Unfortunately, the final solenoid from Table 3.4 was not developed to be submitted to laboratorial tests, the only solenoid that was properly tested was the original prototype with the parameters shown in Table 3.3. The prototype solenoid reached 6.35m/s as maximum speed in the FEMM simulations (Figure 3.28).

To measure speed, a sonar based speed trap was used in a setup that had the two sonars at a distance of 1.3m from each other, taking measurements every 5ms (if the sonars hit a close object, the triggering rate rises). Trying to measure a 6.5m/s ball this way results in errors not greater than 0.16m/s. In our experiences the ball never reaches this velocity, so 0.16m/s is a small error and the method is acceptable.

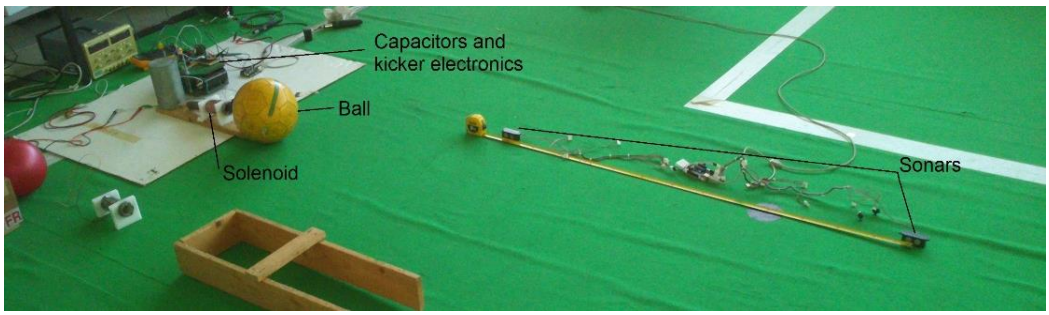

Figure 3.37 - Sonar based speed trap

Using this test bed, the ball was shot several times to study how to achieve best results with the kicker. Some videos can be seen in the Youtube channel created for this thesis [27].

The first thing to find was the correct time of discharge to produce the most powerful shot. Results from Figure 3.38 show that stronger kicks were achieved with a current pulse of $45ms$. This is consistent with equation (*3.11*), the traveling distance is $115mm$, hence $t_f = \frac{2\times0.115}{5.5} = 0.041\ s$.

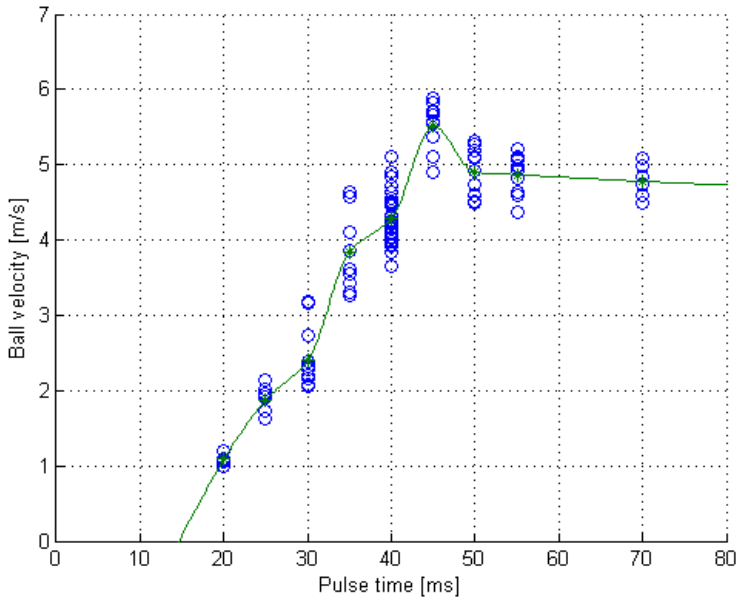

Figure 3.38 - Experimental results for shots varying the current pulse

An average velocity of all shots was calculated and used as the expected velocity for each pulse.

Table 3.5 - Ball velocity vs. pulse time

Pulse time $[ms]$	Ball Velocity $[m/s]$
20	1.09
25	1.88
30	2.40
35	3.85
40	4.13
45	5.51
50	4.90
55	4.87
70	4.78

During this experiment it was noticed that between trials, with all the parameters as close as possible, the ball velocity still varied more than the maximum error expected from the speed trap. The standard deviation for the $45ms$ pulse was $0.31m/s$. This means that the final velocity is very dependable from the geometric factors between ball and kicker.

What gave this difference in strength, could have been slight variations in the position of the ball and rod.

- The rod must hit the center of the ball. If the rod does not hit the center of the ball, the ball is kicked slower, and misaligned.
- For the 45ms pulse to work correctly, the rod must always have the same initial position. This was tested and it was concluded that the best performance is achieved if the rod begins slightly inside the coil. This happens because the capacitors lose voltage during the discharge, and in the initial part of the movement, the forces are not very strong.
- The distance between the ball and the solenoid must always be the same. Shots were made varying the distance between the ball and the rod. It was found that shooting the ball too close to the thrust rod, resulted in lower speeds. And the distance for which the rod collides with maximum speed also was not the best. The best results were when the rod was almost at full speed, in this situation the rod is still receiving force favorable to the movement and shooting the ball has the best results. In all the results from Figure 3.38, the ball was in that optimal position, and that is why the 70ms pulse still has good results, the rod hits the ball before the force becomes negative.

This variations in speed for the same pulse are not problematic when shooting parallel to the ground, but robots from RoboCup are already making use of lob shots and that will require a much more precise kick for the robot to be able to aim correctly.

From Figure 3.38, it can also be seen how easy it is to shoot with different powers. This is one of the advantages of the electromagnetic kicker, i.e., to kick with different ball velocities, with only the adaptation of the current pulse duration.

Another important thing to check is the aim accuracy of the robot/kicker. Shots were made at a target, and knowing the distance to the target, the aim error was calculated. The ball is being shot with a maximum error of 5%. This may be a small error when shooting from close distances but for long shots and passes, more accuracy is needed. A 5% error represents 0.8m of error when shooting from a distance of 9m (midfield to goal). To minimize this error, the position of the ball relative to the kicker must be tighter. The dribbling system should address this problem.

When shooting with the maximum power it was verified that the capacitors discharged to nearly 70V (Figure 3.16), using equation (*3.12*) the energy spent to kick the ball is almost 181J, which is much higher than the energy transmitted to the ball. Using equation (*3.13*), and the weight of the soccer ball (430g), the energy transmitted is $W = \frac{1}{2} \times 0.430 \times 5.5^2 = 6.5J$. This means that the energy transfer efficiency from the capacitors to the ball is very low, inferior to 4%.

Chapter 4

Dribbling System

The dribbling system came into need because the soccer robots must react faster to gameplay situations and also because the kicker system cannot perform a proper kick if the ball is not correctly positioned in front of the robot. In the beginning, MSL robots only used passive systems that relied in path planning strategies, but the robot accuracy, concerning its own position and ball detection, has some error and delay, and this made it difficult for the robot to compensate the movements of the ball with success.

Simple tasks like stopping the ball required the robot to rotate around the ball to push it from the other side. This had to be very fast to be good enough for the current level of the competition, and there is the added problem that opponent robots could block the paths needed to drive the ball.

The very first active dribbler mechanism for soccer robots appeared in 2000, by team Cornell in the small size league. Even for small robots the solution was a drum rotating to pull the ball closer to the robot [28]. These systems, when compared with their passive counterparts, are much more effective and provide a much wider freedom of movement to the robot.

Along this chapter, a cheap motor-based dribbler system will be developed, with the intent of helping the robot drive the ball and perform its main tasks, although it is not expected the same performance as that achieved by state of the art dribbling systems that will also be mentioned in this chapter.

4.1 Theory

The concept of using a motor to control a soccer ball is very easy to understand. If the ball is put in contact with something that has more adherence than between the ball and the floor, the ball will adhere to that surface. If that surface is a wheel controlled by a motor, the rotation of the wheel will force the ball to rotate. For this to happen the wheel must have an adherent surface and the motor must have enough torque to move the weight of the ball and win the friction of the floor.

This is also valid with the constraints of the RoboCup rules that states that the ball can only enter the robot by one third. If the wheel is placed at one third of the ball like in Figure 4.1, the force applied will not have the desired force vector but still has a useful component.

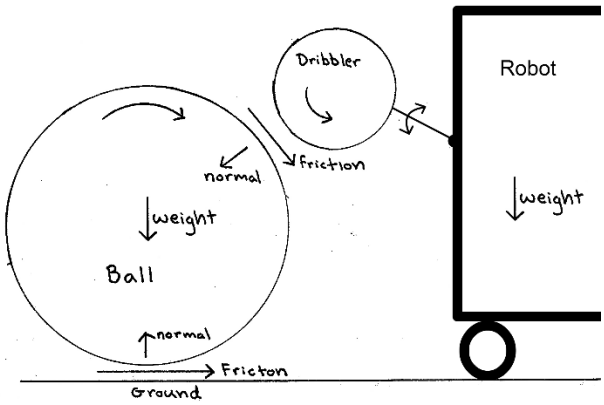

Figure 4.1 - Active dribbler concept, adapted from [28]

The contact between the ball and the dribbler wheel is indispensable for the system to act. The wheel support must have angular movement by means of a hinge, so the ball can stay in contact with the wheel in a wider range of positions. There are several examples of this active dribblers being used in RoboCup, and despite the number of wheels being used, the concept is the same. The use of two wheels gives more points of contact letting the system apply more force to the ball, and the asymmetric action of the wheels gives the ability to force the ball to rotate laterally or dock the ball in front of the robot or any other position if the geometry of the system is designed that way.

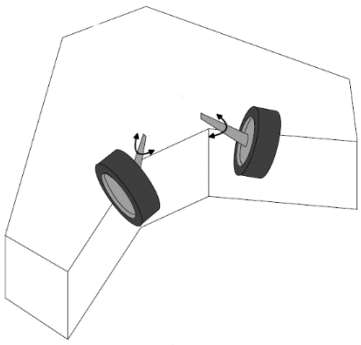

Figure 4.2 - Dribbler configuration with two wheels (adapted from [29])

The active dribbler provides a powerful way of controlling the ball, but as a tradeoff the whole system has to be permanently controlled, because the ball will not move freely when in contact with the robot.

To control the ball and as stated in the rules, keeping it rolling in the direction of the movement, open and/or closed loop controllers must be used.

Controlling the dribbler in open loop is a simple feed forward design with the dribbler matching the robot movement plus an intentional offset. The objective is to keep the ball movement always less than the actual robot velocity. But this kind of control has to be manually adjusted to achieve good performance, giving the user small choice in what the controller does.

On the other hand, a closed loop controller, with the help of additional sensors, can control the ball with much more precision. Inputs like the velocity of the dribbler and the precise position of the ball, can be used in the closed loop controller.

A research from other team in the competition [11], validates the option of controlling the ball only with the feedback controller, but combining the feed-forward controller lets the system react faster to the changes and minimizes the errors controlling the ball.

In either of the controllers, the desired velocities of the wheels are related with the velocity of the robot by a direction dependent gain, this means that when the robot is moving forward, the objective is to make the ball spin slower than the robot movement, keeping it pressed to the robot, and when the robot is moving backwards, the ball must spin more than the velocity of the robot, again keeping it pressed against the robot.

To choose the appropriate motor to dribble the ball some calculations must be done, the motor torque (τ) must overcome the ball rotational inertia [30] which can be calculated by Newton's second law for rotation.

$$\tau = \alpha \times I \;\; ; \;\; \alpha = \frac{a}{r} \tag{4.1}$$

Where, α is the angular acceleration desired, and I is the moment of inertia of a spherical shell which is known to be:

$$I = \frac{2}{3} m r^2 \tag{4.2}$$

The other requirement for the motor is its linear velocity that must be able to match the robot velocity. Thus, the motor rotations per minute (RPM) must be:.

$$RPM = \frac{v}{2\pi r} \times 60 \tag{4.3}$$

For the above equations, a is the acceleration, r is the radius, m is the mass, and v is the velocity.

4.2 Implementation

The objective was to develop a low-cost solution for the dribbling system, so it was chosen to use a design with only one wheel.

The first step was to find a wheel with enough grip to rotate the ball. The chosen wheel is one with 66mm of diameter from Radio-controlled (RC) modeling, which has tires with strong adherence and is very cheap.

Next, the motor to drive the wheel was chosen. The SocRob robots have a maximum speed of nearly 3m/s but at the moment the max speed is reduced by software to 2m/s as an imposition of the RoboCup rules. Using equations (*4.1*)(*4.2*)(*4.3*), the characteristics of the motor are:

$$RPM = \frac{2}{2\pi \times 0.033} \times 60 = 579\text{rpm}$$

And for the torque,

$$I = \frac{2}{3} \times 0.43 \times 0.11^2 = 0.0035\ kg.m^2 \; ; \; \tau = 0.0035 \times \frac{2}{0.11} = 0.063\ N.m$$

Figure 4.3 - Wheel and motor

The chosen motor has characteristics a little below the calculated. This motor is very cheap but it does not include a tachometer or an encoder, this will make it harder to control the ball correctly because there is no feedback about the motor real rotation.

Due to the different application for which the wheel is usually destined, the wheel and the motor did not have a compatible mounting. This was easily solved with a small brass connector designed to connect both parts. Figure 4.3 shows the motor connected to the wheel and Table 4.1 shows the motor characteristics.

Table 4.1 - Dribbler motor parameters

Parameter	**Value**
Voltage [V]	12
RPM	500
Torque [$N.m$]	0.049
Length [mm]	66
Shaft length [mm]	9.5
Shaft diameter [mm]	4
Weight [g]	88

To operate this motor in both directions, an H-bridge circuit is necessary. The UC33886 integrated circuit, from Freescale Semiconductor, was used. The UC33886 is an H-bridge able to control continuous inductive DC load currents up to 5A. The outputs can be controlled by 2 digital signals that choose the direction of rotation and a PWM signal that chooses the speed. These control signals will be provided from the Arduino microcontroller.

Figure 4.4 - H-bridge Board

The dribbler architecture is simple, the laptop chooses the dribbler velocity, and communicates to the microcontroller that will send the signals to the H-bridge controlling the motor.

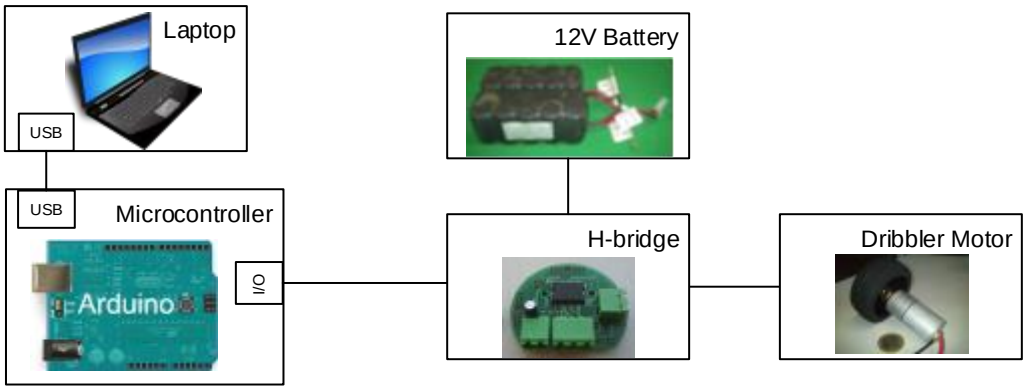

Figure 4.5 - Dribbler architecture diagram

Using Autodesk Inventor and the 3D model of the robot, a support for the motor was designed, and with the help of EDP FabLab, a free self-service workshop outside IST, a 3D printed prototype was done. After testing its correct performance, the sturdier metal counterparts were made, in "*Núcleo de Oficinas* (NOF)", an internal workshop from IST. Detailed designs can be seen in Appendix C.

The support has the required axis for rotational movement, and a prolongation to the back to attach a spring in case it is needed to compensate the weight. Unlike the past system, the adjustment of height is passive. The motor support is detachable to enable the use of different motors.

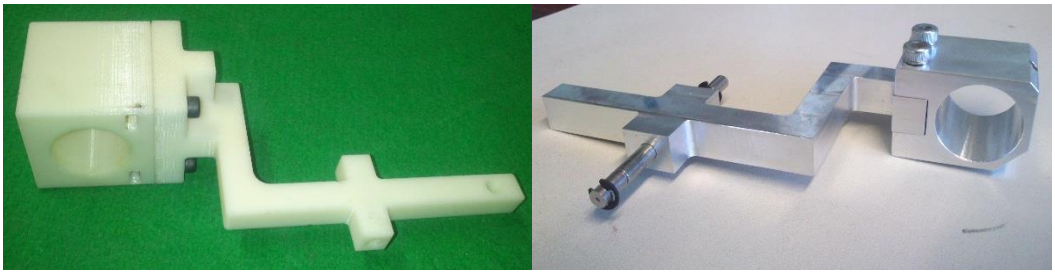

Figure 4.6 - Dribbler support, (left) prototype and (right) final version

The design fitted nicely inside the robot, with the kicker system also already installed.

Figure 4.7 - SocRob robot with ball handling systems installed

In this thesis, the control system for the dribbler will only feed-forward the robot velocity to control the dribbler wheel in an open loop. But the designs were made leaving the option of changing the motor and if other sensors are to be added to the dribbling system, future improvements and different kinds of control can be done.

The low level microcontroller only receives a speed value filtering invalid inputs and sets the wheel to rotate at that speed. All the control implementation, and adjustment is done in the high level code running in the laptop.

As explained in the 4.1, the controller's goal is to slow the ball down when moving forward, and speed the ball up when moving backwards, keeping the ball rotating always in the natural direction of the movement.

4.3 Results

The dribbling performance was measured in two distinct situations.

The first is controlling the robot manually and check at which extent he can drive the ball without losing it.

The second is how the robot performs when running its autonomous behaviors.

This had to be tested separately because there was no time to update all the autonomous behaviors to exploit the dribbler advantages, and some situations worked with manual controls but failed in the behaviors, which means that the problems may be in the behaviors. This section only reports the remote controlled results. The rest will be shown in Chapter 5.

The best way to show this results is through the videos in the Youtube channel. [27]

Without much adaptation of the dribbling control, the robot was able to move forward, backwards and brake without losing the ball.

The best method of control found was to rotate the wheel with the robot velocity minus a constant, in case of moving forward, and rotate the wheel with the robot velocity plus a constant in case the movement was backwards.

The forward movement was stable and did not interfere with the ball natural movement. The action of braking while moving forward had a success rate of 18 out of 20.

The backward movement was also good, sometimes when moving too fast the ball was lost due to the low power motor. This is not a problem because the rules state that the robot can only move backwards for a maximum of 2 meters, so it is not the case that the ball will be lost due to this movement.

Due to the low power motor an advantage was found, the motor does not have the power to force the ball spin back when the robot is stopped, this enables the motor to be in full power when trying to catch balls or when moving backwards because the ball will only rotate with the movement of the robot. This did not cause the motor to heat and is very useful because currently there is no feedback if the robot has the ball or not.

Stronger motors were also tried, to check their performance, but they were incompatible with the rest of the robot electronics, the stronger motors created strong magnetic noise which interfered with

the Inter-Integrated Circuit (I2C) communications of the sensors, in case of needing stronger motors in the future, they will need better magnetic isolation.

Rotating and turning with the ball has a higher percentage of lost balls if these movements are fast, but given that the movements are much harder the results are also good, the dribbler worked well with normal movements. Compared to what the robot used to do without the dribbler, the improvements are big.

Although, the dribbler mechanism is not the only responsible for the lost balls, the geometry of the robot has a flat front, and uses spring “fingers” (shown in Figure 4.7) to keep the ball from drifting away. A closer look at the robot while dribbling the ball shown that when the robot rotated, this springs sometimes fling the ball away. These spring “fingers” are also responsible for bad results when catching the ball, the ball often collides against the “fingers” without letting the dribbler wheel touch the ball.

With the flat front, the dribbler system already lacks physical protection against impacts from other robots, which can cause undesirable plastic deformations or even total fracture of the mechanisms. The developed dribbler system was used in competition during RoboCup 2013, and such damages were observed. The developed structure resisted without problems but the axis of the motor and the robot chassis were slightly damaged.

To solve this, the “fingers” should be substituted by a concave front that would correct the rotation problems as well as protect the dribbling system. This should also influence the problem regarding the kicker aim accuracy reported in 3.2.3

An example was drawn and added to the 3D model for insight.

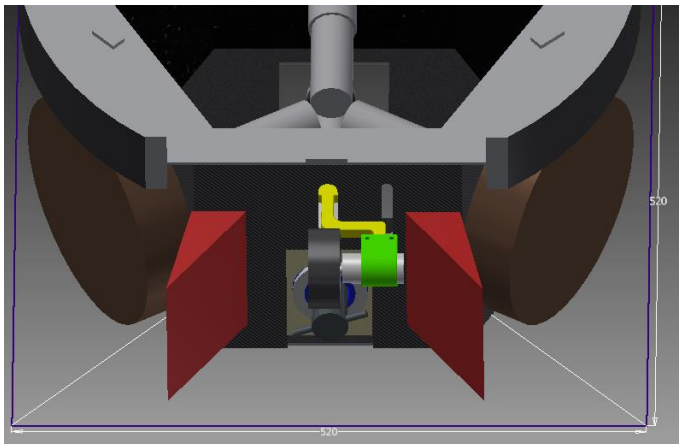

Figure 4.8 - Concept of new robot front

The front of the robot has 90mm of space to use, so it is possible to do a change like in Figure 4.8.

The angle of the structure has to be chosen for best performance, a wider angle would benefit the reception of balls but decreases the rotation and turning ability. A small test using a wooden structure was performed, and showed better results, but it was not built to withstand the impacts expected.

Chapter 5

Case study in a soccer robot

The case study was the integration of both systems in the SocRob team, which was the objective since the beginning.

For a successful integration, the microcontrollers had to be programmed to work together with the robot main code in the laptops.

5.1 Implementation

For the kicker system, given the constraints and danger of misuse, all of the technical decisions as the discharge procedure, kick strengths, charge limits and hysteresis are programmed into the microcontroller. This way, it becomes very simple for the high level to interact with the kicker, only simple commands as “k” to kick, or “c” to start charging, are sent to the microcontroller that takes care of everything else.

A diagram summarizing the microcontroller state machine can be seen in Figure 5.1.

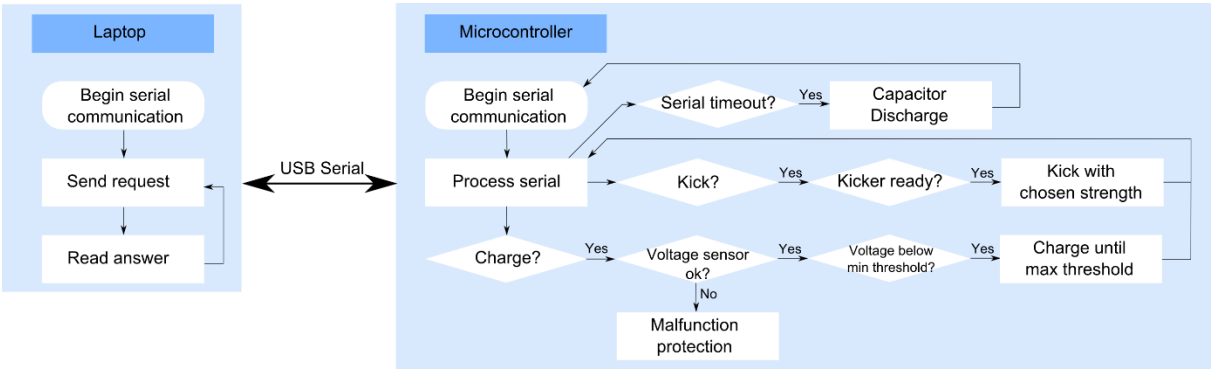

Figure 5.1 - Kicker system control diagram

For the dribbler, the microcontroller is the simplest one. The integration and technical choices are implemented in the main software code, and the microcontroller only actuates over the H-bridge.

The dribbler system was harder to integrate. The motion with and without autonomous behaviors was different. The robot behaviors have a big impact on the dribbler performance, a big difference is the fact that during the dribbler development, the acceleration limits of the robot were critically changed. This changes completely the motion of the robot, and the best way to act upon the ball can change, as it was the case.

Several control methods were tried. Due to the robot acceleration limits, using the final speed value would push the ball away because the dribbler would reach that velocity faster than the robot, and the use of odometry would let the ball escape when decelerating the robot.

Due to the characteristics of the motor, it was possible to control the ball in a much simpler way. When moving backwards, as explained in 4.3, the motor can pull the ball with maximum power, and when moving forward a very low force was applied also rotating backwards, this will make the wheel slow the ball a little and is not strong enough to interfere will the natural movement of the ball.

Surprisingly this method achieved the best results, although, a more complex control scheme that models the robot actions correctly should achieve at least the same results.

During the integration of the dribbler, the ball detection performed by the camera was used as feedback for the dribbler. Figure 5.2 shows the dribbler control diagram.

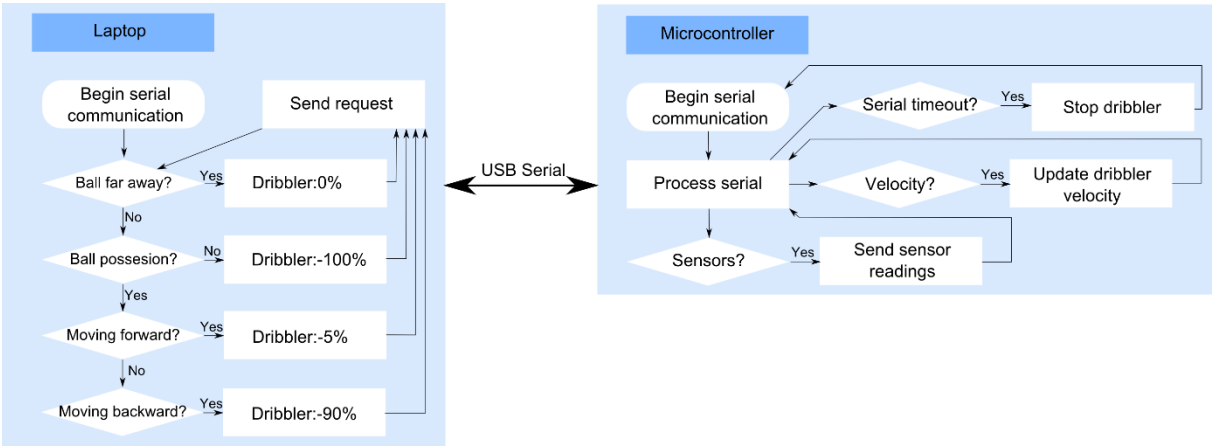

Figure 5.2 - Dribbler system control diagram

Besides the integration with the main software, a standalone graphical user interface was also developed to communicate with the dribbler and the kicker. This interface was written in the Processing programing language [31], because the Arduino language [14] is based on it, and Processing is often used to rapidly create interfaces running on a computer and communicating with the Arduino microcontroller.

Both interfaces can be seen in Figure 5.3, and their purpose is to help the testing and debugging process of the developed systems, isolating the systems from problems in the main software. The remote controlled tests were performed recurring to these interfaces.

Figure 5.3 - Standalone interfaces to test the hardware developed

5.2 Results

Practical tests of both systems working together were carried out, as well as with autonomous behaviors adapted to make use of the new systems. Concerning the dribbler and kicker systems, the same good results as in manual experimentation were observed, but due to the lack of the whole process of robot calibration that is usually performed before competition, the robot autonomous behaviors did not always perform in their best conditions, showing good performance from the systems developed, but sometimes unable to complete the objectives.

The results from the integration can also be seen in the Youtube channel [27].

The test conducted was to run the “BehaviorBaseAttack”, this behavior is a sequence of actions that lead the robot to find and catch the ball, then the robot turns to the opposite goal, and kicks the ball.

The kicker system did not have any difference from the results in section 3.2.3. The main software only needs to send the kick signal and strength to the microcontroller, and the kick is executed if the kicker is ready. Sometimes the kicker tried to shoot and missed the ball, this occurs due to inaccurate knowledge of ball possession. This problem can be solved having a better way of detecting the possession of the ball. The ball position given by the camera has some errors.

Regarding the dribbler system, in first place, the feedback from the camera had to be disabled. As happened with the kicker, the camera detection of the ball has errors, but in the dribbler the consequences were more serious. If the robot tried to dribble the ball forward with the information of not having the ball then the robot would get stuck against the ball.

In the meantime the dribbler works assuming the robot always has the ball. With this change the dribbler worked like in section 4.3. The robot behaviors sometimes improved the dribbler performance. The situation where the dribbler performance was improved was during rotations and turning. The combination of the dribbler system with the previous path planning movements resulted in increased performance. Other times the robot did not get close to the ball for the dribbler to act, due to self-localization and ball detection errors. This means that the robot behaviors and predicates need more adaptation.

The results show that the dribbler can improve performance not only by adapting the dribbler system to the various situations, but as well by adapting the behaviors to the dribbler.

After optimizing the “BehaviorBaseAttack” the robot was able to catch the ball, rotate to the goal without losing the ball, and shoot, scoring a goal. A rate of success was not calculated, because most of the times the robot self-localization was the problem and the rate of success would not represent the performance of the systems developed in this thesis.

Chapter 6

Final Remarks

6.1 Conclusions

This thesis reports the development steps of building new ball handling actuators for a mobile soccer robot.

The original objective of the thesis was accomplished, endowing the SocRob soccer robots with stable kicker and dribbler systems.

For the kicker, the choice was an electromagnetic system. The new power converter has a higher efficiency, recharging the capacitors and enabling a full power kick every 5 seconds. The solenoid equipped in the robot shoots the ball with half the velocity intended (5m/s) but a deep analysis on how to achieve the desired launch velocity (9m/s) was performed and is yet to be implemented in a prototype.

The dribbler system also improved the robot ability to drive the ball through the field, and to keep the ball ready to be shot by the kicker system. The use of only one low-cost motor in the dribbling mechanism was successful and resulted in an efficient dribbling mechanism, leaving room for future improvements.

6.2 Future work

For future work, the implementation of the optimized solenoid, improving the ball launch speed is a must do. With this improvement it will be possible to explore the potential of lob shots. For the lob shots a new mechanical system has to be developed as well. A good option would be a front leg, on which the developed kicker would collide. With the option of moving the leg up and down, the angle at which the ball is fired could be chosen.

Building the frontal protection of the robot also proved to be necessary and should be done for future use.

The new sensors to help detect the ball possession are not critical but would be a good improvement. The auxiliary detection can be achieved through potentiometers attached to the dribbler support like “Tech United” uses, or simply using infrared sensors pointed specifically to detect the ball.

The prototype circuit boards used in this thesis were made out of strip boards. Even though the prototypes are fully functional, for the next robots, they should be redesigned for printed circuit boards (PCB).

The adaptation of the autonomous behaviors must also be done. The pass between robots requires especial attention because the strength of the pass must be chosen according to the conditions.

References

[1] "RoboCup," The RoboCup Federation, [Online]. Available: http://www.robocup.org/.

[2] H.-D. Burkhard, D. Duhaut, M. Fujita, P. Lima, R. Murphy and R. Rojas, "The Road to Robocup 2050," *Robotics & Automation Magazine, IEEE,* vol. 9, pp. 31-38, 2002.

[3] "Robocup Middle Size League Rules," Robocup, 2013 January 16. [Online]. Available: http://wiki.robocup.org/wiki/Middle_Size_League.

[4] S. M. Kasaei, S. M. M. Kasaei and S. M. Kasaei, "Design and Implementation Solenoid Based Kicking Mechanism for Soccer Robot Applied in Robocup-MSL," *International Journal of Advanced Robotic Systems,* Vols. 7, No.4, pp. 73-80, 2010.

[5] Y. Kitazumi, S. Ishida, Y. Ogawa, K. Yamada, Y. Sato, M. Oki, H. Thoriyama, N. Shinpuku, Y. Takemura, A. A. Nassiraei, I. Godler, K. Ishii and H. Miyamoto, "Hibikino-Musashi Team Description Paper," in *Robocup 2009 International Symposium*, 2009.

[6] M. Riedmiller, "Open Source RoboCup MidSizePlatform," Albert-Ludwigs-Universität Freiburg;HARTING Technologiegruppe;Deutsche Forschungsgemeinschaft, 2011. [Online]. Available: http://ml.informatik.uni-freiburg.de/pub/dfg/doku.php.

[7] A. A. Nassiraei, S. Ishida, N. Shinpuku, M. Hayashi, N. Hirao, K. Fujimoto, K. Fukuda, K. Takanaka, I. Godler, K. Ishii and H. Miyamoto, "Hibikino-Musashi Team Description Paper," Kyushu Institute of Technology, The University of Kitakyushu, Japan, 2013.

[8] K. J. Meessen, J. J. H. Paulides and E. A. Lomonova, "A Football Kicking High Speed Actuator for a Mobile Robotic Application," in *IECON 2010 - 36th Annual Conference on IEEE Industrial Electronics Society*, Glendale, AZ, 2010.

[9] "CAMBADA Robotic Soccer," University of Aveiro, 2013. [Online]. Available: http://robotica.ua.pt/CAMBADA/.

[10] "Tech United Eindhoven," Eindhoven University of Technology, 2013. [Online]. Available: http://www.techunited.nl/.

[11] J. d. Best and M. S. René van de Molengraft, "A novel ball handling mechanism for the RoboCup middle size league," *Mechatronics,* Vols. 21, Issue 2, pp. 469-478, march 2011.

[12] F. Schoenmakers, G. Koudijs, C. L. Martinez, M. Briegel, H. v. Wesel, J. Groenen, O. Hendriks, O. Klooster, R. Soetens and M. v. d. Molengraft, "Tech United Eindhoven Team Description Paper," Eindhoven University of Technology, The Netherlands, 2013.

[13] "OmniISocRob," Institute for Systems and Robotics - Lisbon, [Online]. Available: http://socrob.isr.ist.utl.pt/omnis2006.php.

[14] "Arduino," 2013. [Online]. Available: http://arduino.cc/en/Main/arduinoBoardDuemilanove.

[15] J. Paul, "Coilgun Systems," Coilgun Systems, 2001-2006. [Online]. Available: http://www.coilgun.eclipse.co.uk/coilgun_basics_1.html.

[16] N. Mohan, "Power Electronics and Drives," Minneapolis, MNPERE, 2003.

[17] "POWERSIM," Powersim Inc., [Online]. Available: http://powersimtech.com/products/psim/.

[18] "Wikipedia - Operational Amplifier," Wikimedia Foundation, Inc, [Online]. Available: http://en.wikipedia.org/wiki/Operational_amplifier#Non-inverting_amplifier.

[19] "Fritzing," University of Applied Sciences Potsdam, [Online]. Available: http://fritzing.org/.

[20] L. T. George Proctor, "MachineDesign," 24 January 2008. [Online]. Available: http://machinedesign.com/news/linear-actuators-get-servo-look.

[21] C. R. Nave, "HyperPhysics," Georgia State University, 2013. [Online]. Available: http://hyperphysics.phy-astr.gsu.edu/hbase/magnetic/elemag.html.

[22] B. Hansen, "Barry's Coilgun Design Site," 2013. [Online]. Available: http://www.coilgun.info/femm/home.htm.

[23] B. v. Goch, "Optimizing a solenoid for a RoboCup kicker," Technische Universiteit Eindhoven, Eindhoven, 2006.

[24] J. P. E. Antunes, "Hardware Architecture and Fast Deployment Methods for Soccer Robots," Instituto Superior Técnico, Lisboa, 2009.

[25] D. Meeker, "Finite Element Method Magnetics," 1999. [Online]. Available: http://www.femm.info.

[26] D. Meeker, "Finite Element Method Magnetics : Coilgun," June 2004. [Online]. Available: http://www.femm.info/wiki/CoilGun.

[27] M. S. Serafim, "Msc Thesis Youtube Channel," 13 10 2013. [Online]. Available: http://www.youtube.com/channel/UC2nBSUJ7UHt8D_BS2pTqfTA/videos.

[28] S. Stancliff, *Evolution of Active Dribbling Mechanisms,* 2005.

[29] R. Hoogendijk, M. J. G. v. d. Molengraft, W. H. T. M. Aangenent and R. J. E. Merry, "Design of a Ball Handling," Technische Universiteit Eindhoven, Eindhoven, 2007.

[30] C. R. Nave, "Hyperphysics," Georgia State University, 2013. [Online]. Available: http://hyperphysics.phy-astr.gsu.edu/hbase/inecon.html.

[31] C. R. Ben Fry, "Processing 2," 2013. [Online]. Available: http://processing.org/.

Appendix

A. *MATLAB/FEMM simulation script*

```
%%%%%%%%%%%%%%%%%%%%%%%%%%%%%%%%%%%%%%%%%%%%%%%%%%%%%%%%%%%%%%%%%%%%%%%%%%%%%%%
%AUTHOR: Miguel Santos Serafim
%Description: Simulation of the final solenoid with all the improvements
%             studied
%%%%%%%%%%%%%%%%%%%%%%%%%%%%%%%%%%%%%%%%%%%%%%%%%%%%%%%%%%%%%%%%%%%%%%%%%%%%%%%
%% Section to draw the problem geometry.
%%%%%%%%%%%%%%%%%%%%%%%%%%%%%%%%%%%%%%%%%%%%%%%%%%%%%%%%%%%%%%%%%%%%%%%%%%%%%%%

% The package must be initialized with the openfemm command.
% This command starts up a FEMM process and connects to it
%addpath('c/…/octavefemm/mfiles');
openfemm;

% We need to create a new Magnetostatics document to work on.
newdocument(0);

% PREPROCESSING
% Define the problem type.  Magnetostatic; Units of mm; Axisymmetric;
% Precision of 10^(-8) for the linear solver; a placeholder of 0 for
% the depth dimension, and an angle constraint of 30 degrees
mi_probdef(0, 'millimeters', 'axi', 1.e-8, 0, 30);



% Draw a rectangle for the steel bar on the axis;
% Select the segments and mark them as part of group 1
mi_drawrectangle([0 95; 14 225]);
mi_selectsegment(0,110);
mi_setsegmentprop('<none>',0,1,0,1);
mi_selectsegment(14,110);
mi_setsegmentprop('<none>',0,1,0,1);
mi_selectsegment(5,95);
mi_setsegmentprop('<none>',0,1,0,1);
mi_selectsegment(5,245);
mi_setsegmentprop('<none>',0,1,0,1);

% Draw a rectangle for the tube;
mi_drawrectangle([14.5 -65; 16 65]);

% Draw a rectangle for the coil;
mi_drawrectangle([16 -65; 21 65]);

% Draw the Magnetic Shell tube and washers
mi_drawrectangle([18 71; 27 66]);
mi_drawrectangle([18 -71;27 -66]);
mi_drawrectangle([22 66;27 -66]);

% Draw a half-circle to use as the outer boundary for the problem
mi_drawarc([0 -270; 0 270], 180, 2.5);
mi_addsegment([0 -270; 0 270]);



% Add block labels
% Steel ROD
mi_addblocklabel(5,110);
% Nylon tube
mi_addblocklabel(15,0);
```

```
% Copper coil
mi_addblocklabel(20,-20);
% Air
mi_addblocklabel(40,150);
%Steel shell
mi_addblocklabel(25,70);
mi_addblocklabel(25,-70);
mi_addblocklabel(25,-40);


% Define an "asymptotic boundary condition" property.  This will mimic
% an "open" solution domain
muo = pi*4.e-7;
mi_addboundprop('Asymptotic', 0, 0, 0, 0, 0, 0, 1/(muo*0.2), 0, 2);

% Apply the "Asymptotic" boundary condition to the arc defining the
% boundary of the solution region
mi_selectarcsegment(270,0);
mi_setarcsegmentprop(2.5, 'Asymptotic', 0, 0);

% Add some materials properties
mi_addmaterial('Air', 1, 1, 0, 0, 0, 0, 0, 1, 0, 0, 0);
mi_addmaterial('Coil', 1, 1, 0, 0, 58, 0, 0, 1, 0, 0, 0);
mi_getmaterial('1020 Steel');
mi_addmaterial('Nylon', 1, 1, 0, 0, 0, 0, 0, 1, 0, 0, 0);

% The coil resistance must be calculated to know the current
wire_resistance=20.95;
radius=0.02;
Nlayers=4;
TurnsLayer=110;
V=85;

R=(wire_resistance*2*pi*radius*Nlayers*TurnsLayer)/1000;
IL=V/R;
% IL=73.4

% Set the current passing in the coil
mi_addcircprop('icoil', 73.4, 1);


% match materials and blocks
mi_selectlabel(5,110);
mi_setblockprop('1020 Steel', 0, 1, '<None>', 0, 1, 0);
mi_clearselected

mi_selectlabel(15,0);
mi_setblockprop('Nylon', 0, 1, '<None>', 0, 0, 0);
mi_clearselected

mi_selectlabel(20,-20);
mi_setblockprop('Coil', 0, 1, 'icoil', 0, 0, 440);
mi_clearselected

mi_selectlabel(40,150);
mi_setblockprop('Air', 0, 1, '<None>', 0, 0, 0);
mi_clearselected

mi_selectlabel(25,70);
```

```
mi_setblockprop('1020 Steel', 0, 1, '<None>', 0, 0, 0);
mi_clearselected
mi_selectlabel(25,-70);
mi_setblockprop('1020 Steel', 0, 1, '<None>', 0, 0, 0);
mi_clearselected
mi_selectlabel(25,-40);
mi_setblockprop('1020 Steel', 0, 1, '<None>', 0, 0, 0);
mi_clearselected

mi_zoomnatural
mi_saveas('inductor1.fem');

%%%%%%%%%%%%%%%%%%%%%%%%%%%%%%%%%%%%%%%%%%%%%%%%%%
%% Section to Simulate the forces in the ROD TESTE
%%%%%%%%%%%%%%%%%%%%%%%%%%%%%%%%%%%%%%%%%%%%%%%%%%

%POSTPROCESSING
mi_seteditmode('group');

%center of ROD goes from -160mm to 0mm
for i = 1:33
    Z(i)=(33-i)*(-5);

    % Run the magnetic simulation
    mi_analyze;
    mi_loadsolution;

    % Select block/group 1
    mo_groupselectblock(1);

    % Calculate the z part of steady-state weighted stress tensor force
    F(i)= mo_blockintegral(19);

    % Select group 1 and apply translation
    mi_selectgroup(1);
    mi_movetranslate(0,-5);
end
% Change the force signal
F=F*-1;

%%%%%%%%%%%%%%%%%%%%%%%%%%%%%%%%%%%%%%%%%%%%%%%%%%%%%%%%%%%%%%%%%%
%% Section to Calculate the kinetic energy and velocity of the Rod
%%%%%%%%%%%%%%%%%%%%%%%%%%%%%%%%%%%%%%%%%%%%%%%%%%%%%%%%%%%%%%%%%%

% distance of each translation
d=0.005;
% Work-Energy principle
W=F*d;

% Calculate Kinetic Energy (KE)
for i=1:32
    KE(1)=W(1);
    KE(i+1)=W(i+1)+KE(i);
end

%Estimated weight of the ROD
m100=0.7;
m130=0.850;
```

```
%calculate Velocity
V=sqrt(KE*2/m130);

%%%%%%%%%%%%%%%%%%%%%%%%%%%%%%
%% Section to Plot the Results
%%%%%%%%%%%%%%%%%%%%%%%%%%%%%%

[AX,H1,H2] = plotyy(Z,KE,Z,F);
hold on
plot (Z,V,'r')
set(get(AX(2),'Ylabel'),'String','Force [N]')
ylabel ('Energy [J] and Velocity [m/s]')
xlabel ('Rod position [mm]')
grid on
```

B. Kicker Designs

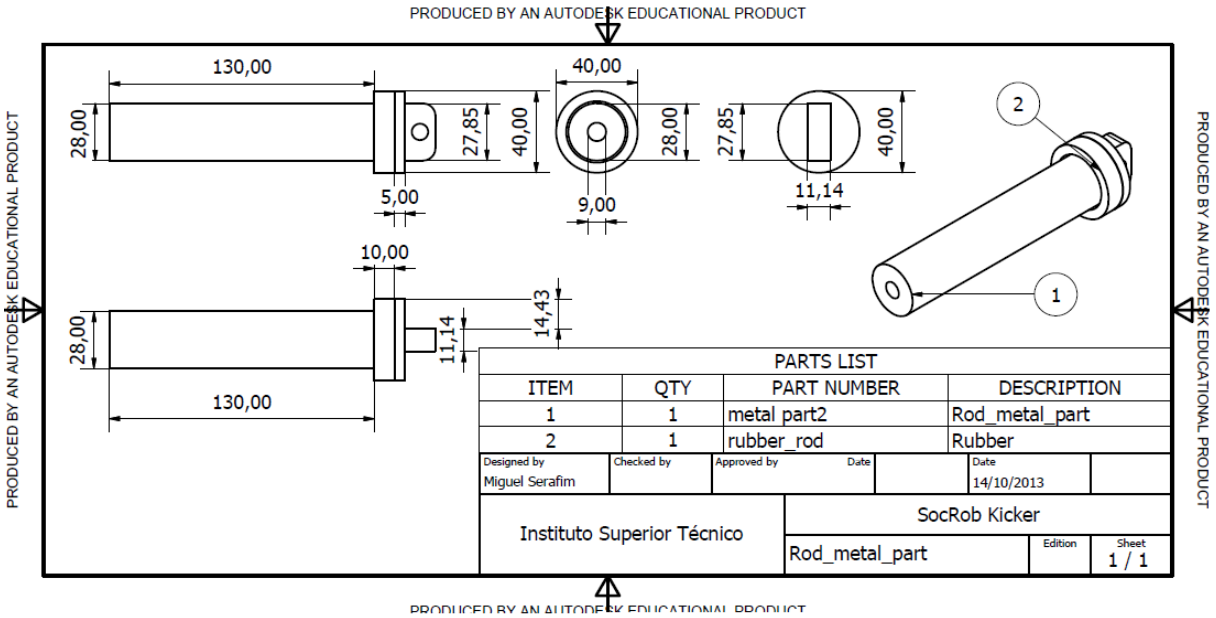

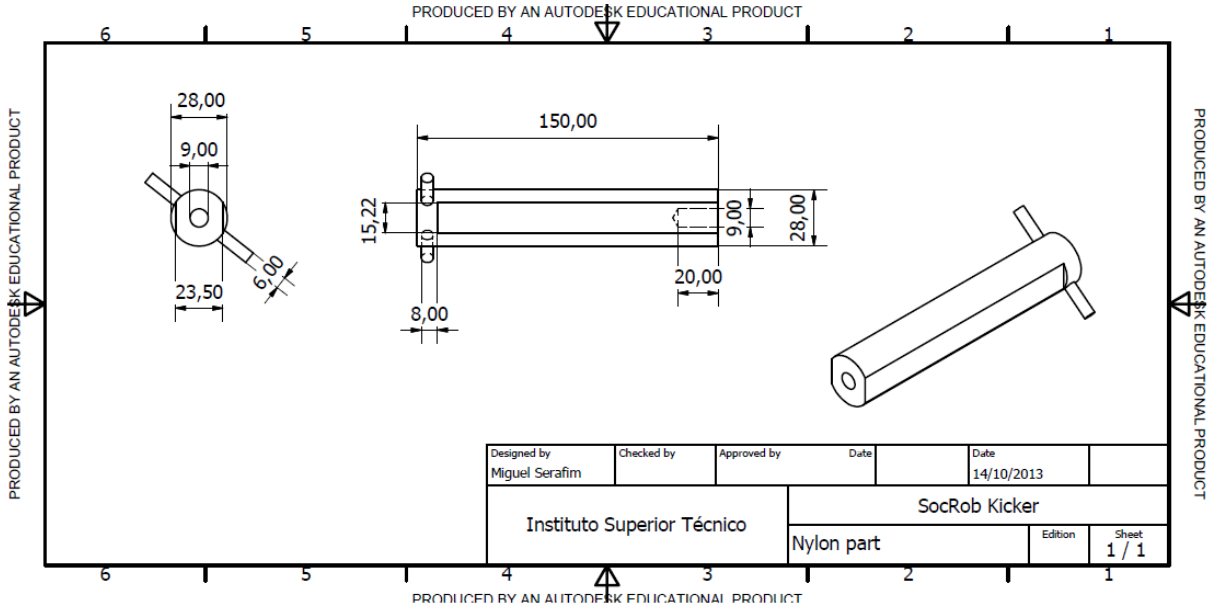

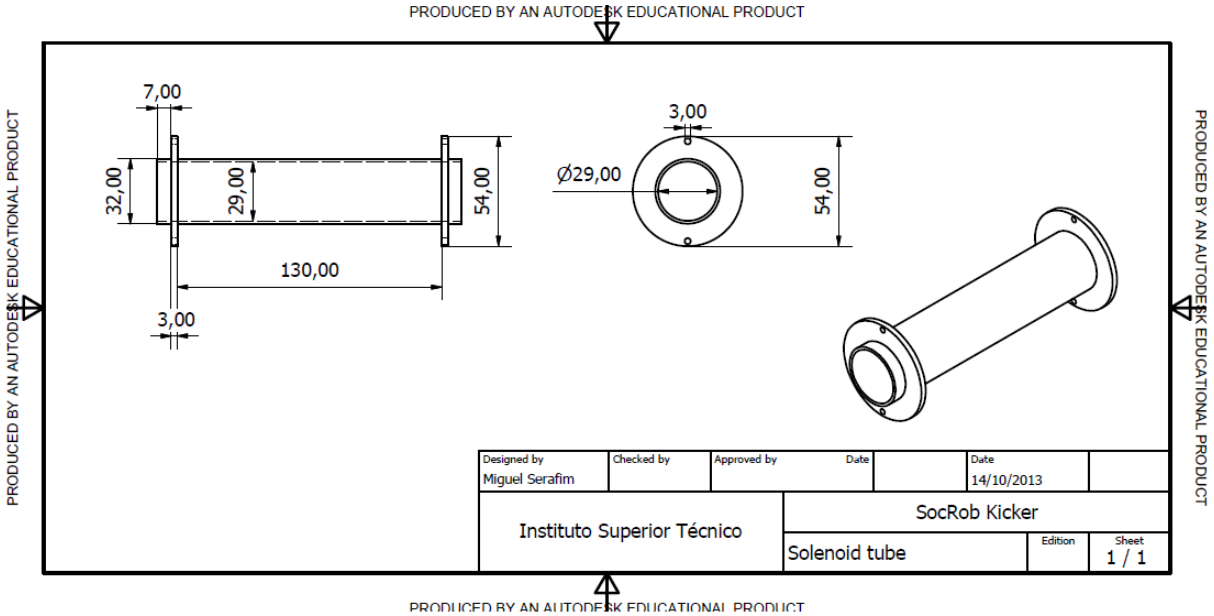
PRODUCED BY AN AUTODESK EDUCATIONAL PRODUCT
7,00
32,00
29,00
54,00
130,00
3,00
3,00
Ø29,00
54,00
Designed by
Miguel Serafim
Checked by
Approved by
Date
Date
14/10/2013
Instituto Superior Técnico
SocRob Kicker
Solenoid tube
Edition
Sheet
1 / 1

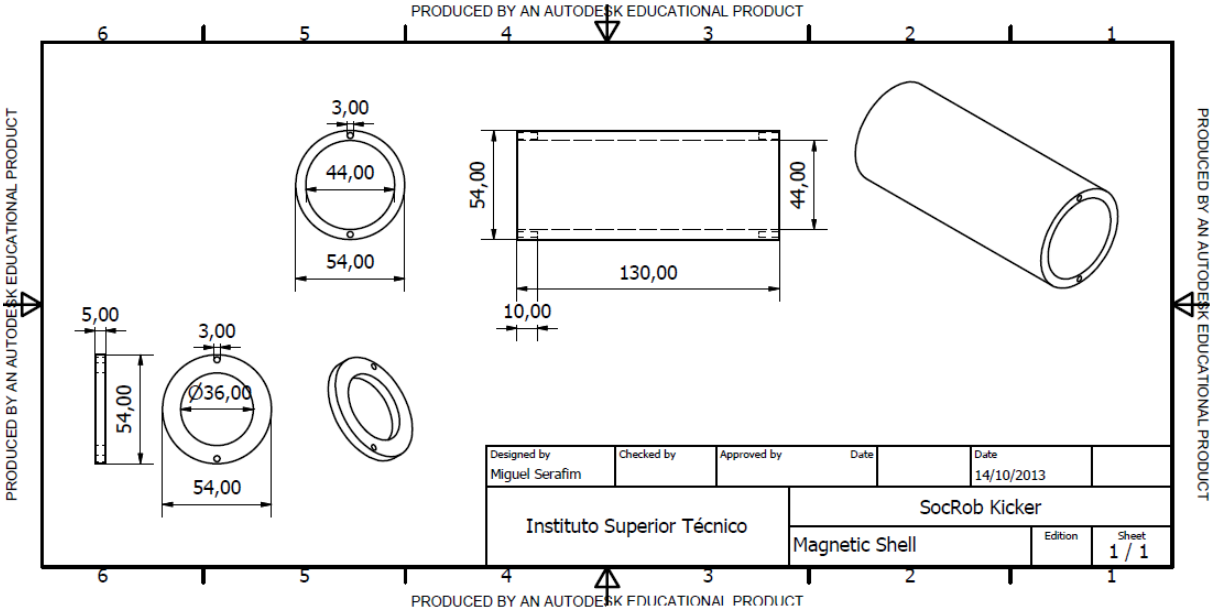
PRODUCED BY AN AUTODESK EDUCATIONAL PRODUCT
3,00
44,00
54,00
54,00
44,00
130,00
10,00
5,00
54,00
3,00
Ø36,00
54,00
Designed by
Miguel Serafim
Checked by
Approved by
Date
Date
14/10/2013
Instituto Superior Técnico
SocRob Kicker
Magnetic Shell
Edition
Sheet
1 / 1

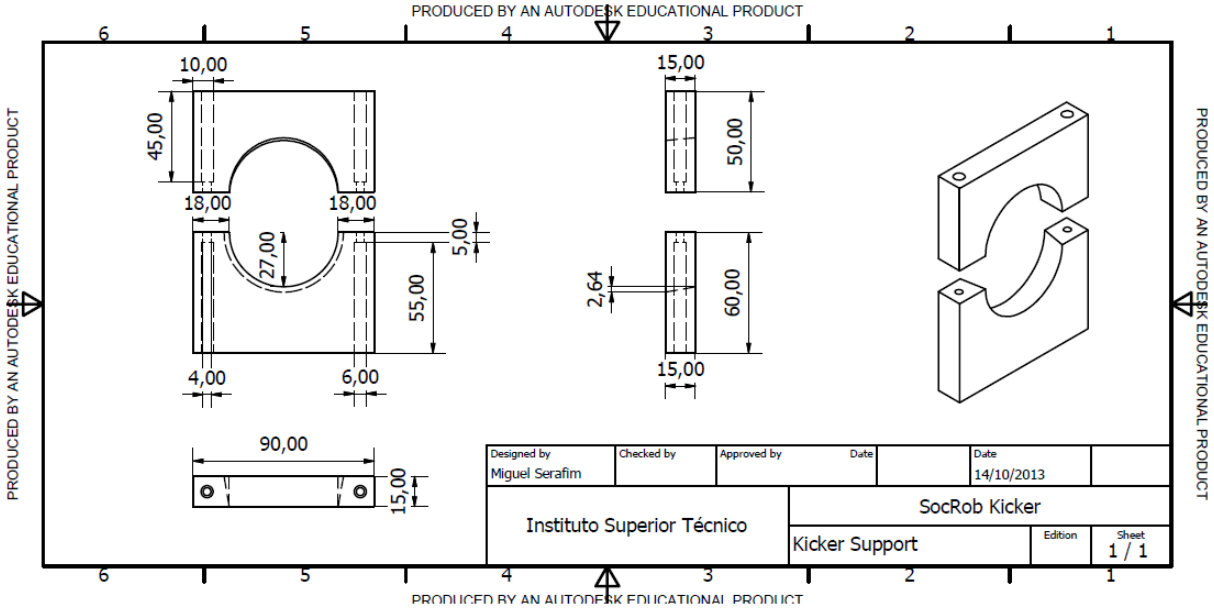
PRODUCED BY AN AUTODESK EDUCATIONAL PRODUCT
10,00
45,00
18,00
18,00
27,00
5,00
55,00
4,00
6,00
90,00
15,00
15,00
50,00
2,64
60,00
15,00
Designed by
Miguel Serafim
Checked by
Approved by
Date
Date
14/10/2013
Instituto Superior Técnico
SocRob Kicker
Kicker Support
Edition
Sheet
1 / 1

C. Dribbler Designs

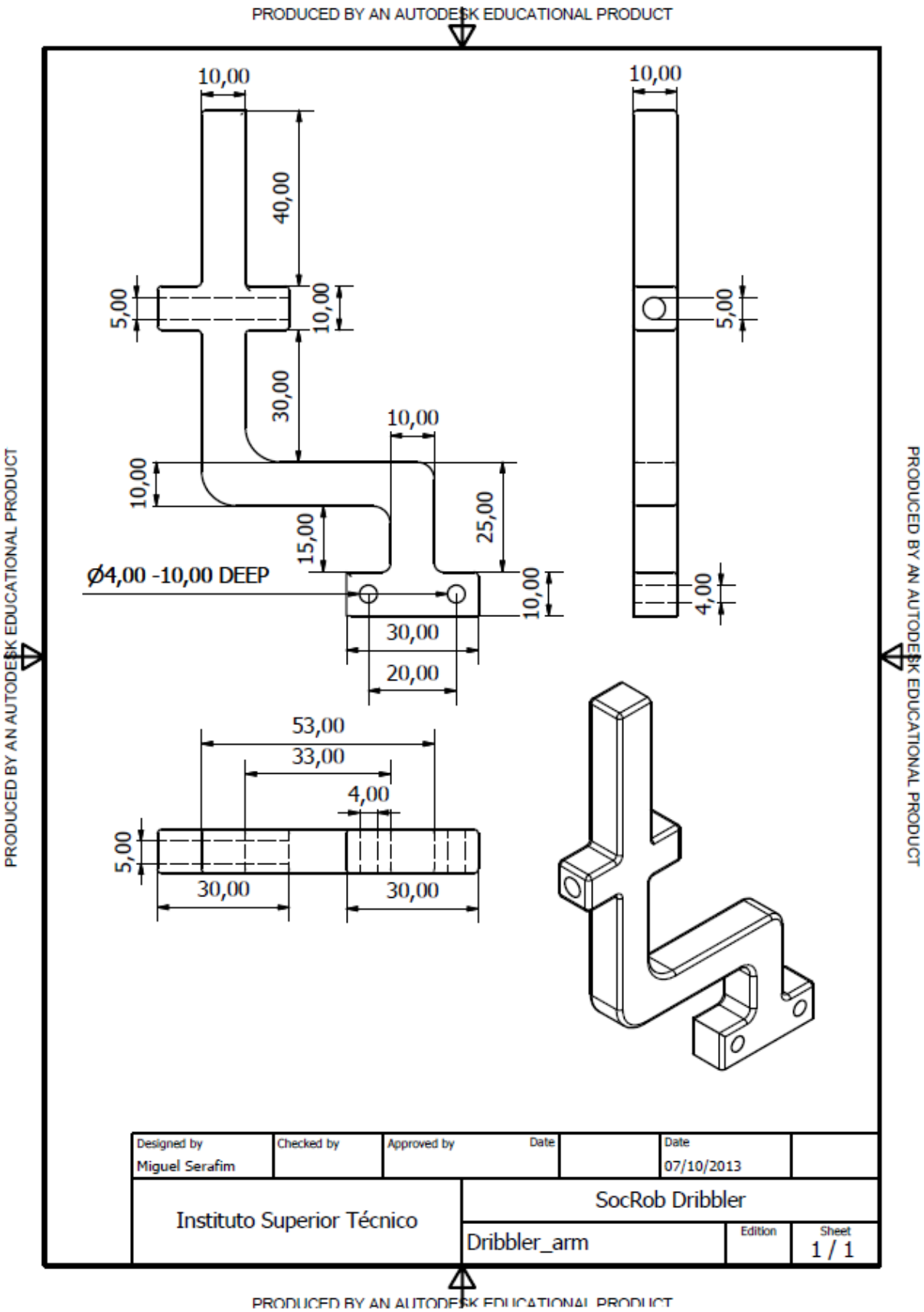

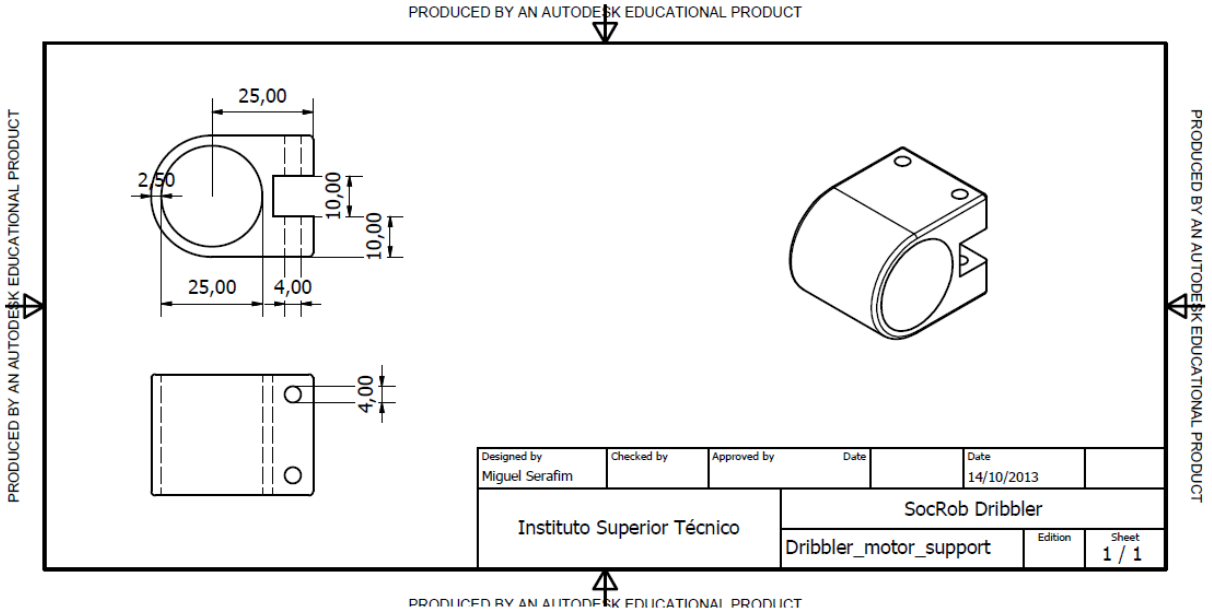
PRODUCED BY AN AUTODESK EDUCATIONAL PRODUCT
25,00
2,50
10,00
10,00
25,00
4,00
4,00
Designed by
Miguel Serafim
Checked by
Approved by
Date
Date
14/10/2013
Instituto Superior Técnico
SocRob Dribbler
Dribbler_motor_support
Edition
Sheet
1 / 1

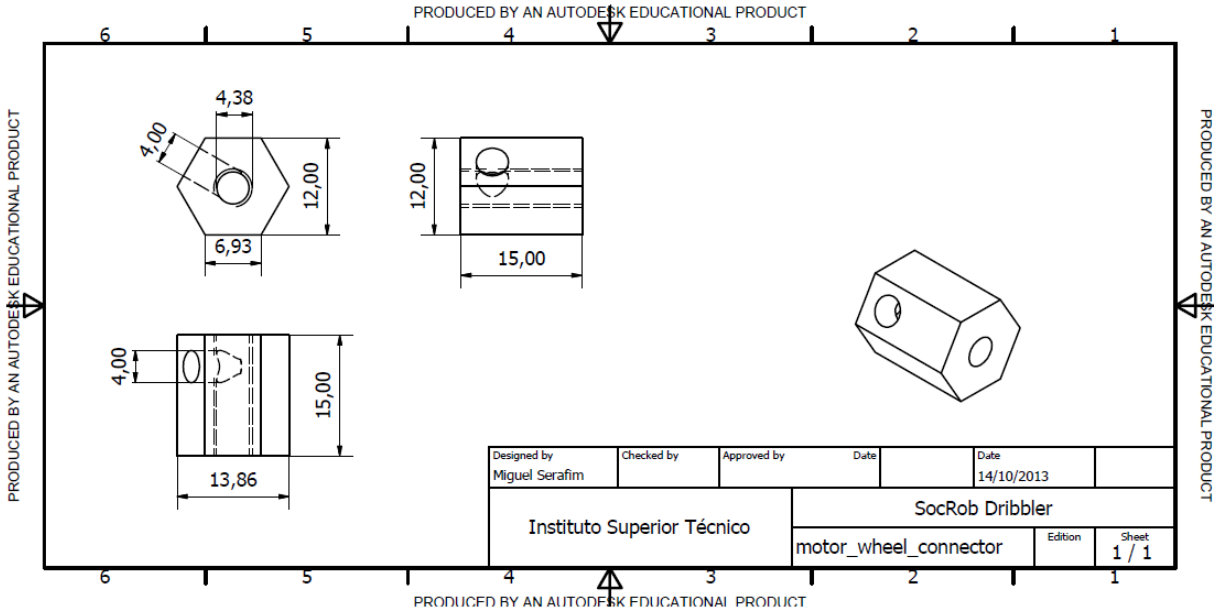
PRODUCED BY AN AUTODESK EDUCATIONAL PRODUCT
4,38
4,00
12,00
6,93
12,00
15,00
4,00
15,00
13,86
Designed by
Miguel Serafim
Checked by
Approved by
Date
Date
14/10/2013
Instituto Superior Técnico
SocRob Dribbler
motor_wheel_connector
Edition
Sheet
1 / 1